Title: Improving disease resistance in plants by editing the epigenome

Authors: Kira M. Veley[1], Kiona Elliott[1,2], Greg Jensen[1], Zhenhui Zhong[3], Suhua Feng[3,4], Marisa Yoder[1], Kerrigan B. Gilbert[1], Jeffrey C. Berry[1], Basudev Ghoshal[3]†, Javier Gallego-Bartolomé[3]‡, Joanna Norton[4], Sharon Motomura-Wages[4], James C. Carrington[1], Steven E. Jacobsen[3,5,6]*, Rebecca S. Bart[1]*

Affiliations:

[1]Donald Danforth Plant Science Center; Saint Louis, MO 63132, USA.

[2] Division of Biological and Biomedical Sciences, Washington University in Saint Louis, Saint Louis, MO, 63110, USA.

[3]Department of Molecular, Cell and Developmental Biology, University of California at Los Angeles; Los Angeles, CA, 90095, USA.

[4]College of Tropical Agriculture & Human Resources, University of Hawaii at Manoa, Hilo, HI, 96720, USA.

[5]Eli & Edythe Broad Center of Regenerative Medicine & Stem Cell Research, University of California at Los Angeles; Los Angeles, CA, 90095, USA.

[6]Howard Hughes Medical Institute, University of California at Los Angeles; Los Angeles, CA, 90095, USA.

*Co-corresponding authors. Email: SEJ: jacobsen@ucla.edu; RSB: rbart@danforthcenter.org

†Current address: Summerland Research and Development Centre, Agriculture and Agri-Food Canada, Summerland, BC, V0H 1Z0, Canada.

‡Current address: Instituto de Biología Molecular y Celular de Plantas (IBMCP), CSIC-Universidad Politécnica de Valencia, 46011 Valencia, Spain.

Abstract:

Pathogens rely on expression of host susceptibility (S) genes to promote infection and disease. As DNA methylation is an epigenetic modification that affects gene expression, blocking access to S genes through targeted methylation could increase disease resistance. *Xanthomonas axonopodis* pv. *manihotis*, the causal agent of cassava bacterial blight (CBB), uses transcription activator-like20 (TAL20) to induce expression of the S gene *MeSWEET10a*. We directed methylation to the TAL20 effector binding element within the *MeSWEET10a* promoter using a synthetic zinc-finger DNA binding domain fused to a component of the RNA-directed DNA methylation pathway. We demonstrate that this methylation prevents TAL20 binding, blocks transcriptional activation of *MeSWEET10a in vivo* and that these plants display increased resistance to CBB while maintaining normal growth and development. This work establishes epigenome editing as a new strategy for crop improvement.

One-Sentence Summary:

Improving disease resistance with epigenomic editing.

Main Text:

Susceptibility (S) genes present a liability within a host genome, as their exploitation is a common mechanism used by diverse classes of pathogens (*1*). In many cases, pathogens actively upregulate expression of S genes during infection. Plant pathogenic bacteria within the *Xanthomonas* and *Ralstonia* genera express transcription activator-like (TAL) effectors that activate transcription of S genes by recognizing and binding specific, largely predictable, promoter sequences (effector binding elements, EBEs) within the host genome (*2–6*). Preventing the exploitation of S genes through genetic modification is one potentially powerful way to engineer resistance (*7–11*). However, removing or altering the genomic sequence at these loci may have negative consequences as these genes are often necessary for normal plant growth and reproductive development (*2*, *12–14*). Alternatively, epigenomic modifications can influence gene expression while leaving genomic sequences intact. Because TAL binding can be inhibited by DNA methylation (*15*, *16*), we hypothesized that targeting methylation to TAL EBEs could be a viable strategy for improving bacterial disease resistance.

In eukaryotes, cytosine DNA methylation is an important mechanism of epigenetic gene regulation (*17*). In plants, the RNA-directed DNA methylation (RdDM) pathway is responsible for establishing *de novo* 5-methylcytosine methylation. Previous targeted methylation efforts leveraged naturally occurring epialleles from Arabidopsis that affect flowering time (*18*, *19*). These studies used CRISPR-Cas9-based tools combined with components of the methylation pathways, either the catalytic domain of the plant methyltransferase DOMAINS REARRANGED METHYLTRANSFERASE 2 (DRM2) involved in RdDM or the bacterial CG-methyltransferase MQ1 (*20*, *21*). In addition, a number of RdDM proteins are effective in targeting methylation when fused with artificial zinc-fingers (ZFs), including DRM2 and

DEFECTIVE IN MERISTEM SILENCING 3 (DMS3), a protein that in Arabidopsis targets RNA polymerase V binding to chromatin to trigger RdDM (*22*, *23*).

Cassava bacterial blight (CBB) is caused by *Xanthomonas axonopodis* pv. *manihotis* (*Xam, aka. Xanthomonas phaseoli* pv. *manihotis* (*24*)) and occurs in all regions where cassava (*Manihot esculenta* Crantz) is grown (*25*, *26*). Symptoms of an infection begin with dark green, angular, "water-soaked" lesions on leaves (Fig. 1A) after which *Xam* moves through the vasculature causing leaf wilting and eventual death of the plant. *Xam* secretes 20 - 30 effectors, including multiple TAL effectors, into cassava cells (*27*). One of these TAL effectors, TAL20, induces ectopic S gene expression of a SWEET (Sugars Will Eventually be Exported Transporters) family sugar transporter, *MeSWEET10a* (*3*, *28*). Expression of *MeSWEET10a* during infection is required for water-soaking phenotypes and full virulence (*3*). Our previous work characterizing the epigenome of cassava revealed that in wild-type cassava, the promoter of *MeSWEET10a* is not methylated (*29*). Thus, we hypothesized that targeted methylation at the TAL20 EBE would prevent ectopic expression of *MeSWEET10a* and provide resistance to CBB (Fig 1B).

We first tested the effect of methylation on TAL20 binding to the EBE *in vitro* using an Electrophoretic Mobility Shift Assay (EMSA) (Fig. S1). As shown previously (*3*), purified 6xHis-TAL20$_{Xam668}$ binds the unmethylated EBE oligo (lane 2) and, as expected, providing an excess of unlabeled, unmethylated oligo outcompeted for binding (lane 5). Conversely, 6xHis-TAL20$_{Xam668}$ does not efficiently bind the methylated oligo (lane 3), nor did the methylated oligo compete for TAL20 binding, even when supplied in excess (lanes 6 and 7). Therefore, the EBE of *MeSWEET10a* was deemed a good candidate for engineering epigenetic disease resistance. Of the RdDM factors tested in *Arabidopsis thaliana*, DMS3 was shown to be the most effective at delivering methylation to a given locus (*23*). Transgenic cassava plants were generated

expressing an artificial ZF targeting the EBE of *MeSWEET10a* fused to Arabidopsis DMS3 (Fig. 2A, Fig. S2-S7). The targeted region of the *MeSWEET10a* promoter was assessed for methylation using amplicon-based bisulfite sequencing (ampBS-Seq) (Fig. 2B, Fig. S2-S7). Plants expressing the ZF alone showed no methylation at or around the EBE of *MeSWEET10a*. In contrast, all plants expressing DMS3-ZF contained high levels of ectopic CpG methylation within and near the ZF target, including the only two CpG sites within the EBE (Fig. 2B, Fig. S2-S7). Plant phenotypes were evaluated under greenhouse and field conditions using our standard methods (see methods for details). These analyses indicate that methylation did not affect root and shoot growth and development (Fig. 2C, Fig. S8). Whole Genome Bisulfite Sequencing (WGBS) was used to assess specificity of the DMS3-ZF. High levels of *de novo* DNA methylation were observed within the target region, similar to the ampBS-seq result (Fig 2B, Fig. 3A), while DNA methylation within an extended region of 5 kb on either side was comparable between the DMS3-ZF-expressing lines and the ZF alone control (Fig. 3A, B). Additionally, CG, CHG, and CHH methylation across all chromosomes, as well as within genes, was similar between the DMS3-ZF-expressing lines and ZF alone control (Fig. 3C, D, Fig. S9). These results demonstrate a high level of specificity for targeted DMS3-ZF-mediated methylation in cassava.

We next tested the hypothesis that CpG methylation at the TAL20 EBE would prevent activation of *MeSWEET10a in vivo*. Compared to controls, plants from independent DMS3-ZF-expressing lines showed a significant lack of *MeSWEET10a* induction in response to *Xam* infection (Fig. 4A). The suppression of *MeSWEET10a* induction occurred in independently derived transgenic lines and across independent experiments and regardless of the expression level of DMS3-ZF (Fig. S10). These data indicate that methylation prevents activation of *MeSWEET10* expression.

To quantify the effect of methylation at the *MeSWEET10a* EBE on CBB disease *in vivo*, we measured "water-soaked" lesions (Fig. 1A, Fig. 4B, Fig. S11), which are the most obvious early disease symptom and requires induction of *MeSWEET10a* (*3*, *30*). Quantitative analysis of images from *Xam*-infiltrated leaves revealed that plants with methylation at the EBE had a reduced infected area compared to wild-type (Fig. 4C). Further, the area of infection in DMS3-ZF leaves was comparable to leaves infected with *Xam* lacking TAL20 (XamΔTAL20). In addition to a decrease in lesion size, the intensity of water-soaking at and around the infiltration site was also reduced in EBE methylated plants. Grey-scale values from images of lesions were compared to mock-inoculated sites on the same leaf, where more water-soaking equates to a darker appearance. Water-soaking intensity was reduced in plants with methylation at the EBE (Fig. 4D). These results demonstrate that methylation of the EBE site within the promoter of the S gene *MeSWEET10a* results in a gain of resistance to CBB.

In conclusion, we show that DMS3 paired with an artificial ZF caused targeted, *de novo* establishment of methylation at the EBE of *MeSWEET10a,* blocking TAL20-induced ectopic expression of *MeSWEET10a* and resulted in gain of resistance to CBB. This represents the first plant resistance allele generated via targeted changes in methylation. More broadly, this work establishes epigenomic editing as a new approach for plant engineering and crop improvement.

References and Notes

1. C. C. N. van Schie, F. L. W. Takken, Susceptibility genes 101: how to be a good host. *Annu Rev Phytopathol*. **52**, 551–581 (2014).

2. G. Antony, J. Zhou, S. Huang, T. Li, B. Liu, F. White, B. Yang, Rice xa13 Recessive Resistance to Bacterial Blight Is Defeated by Induction of the Disease Susceptibility Gene Os-11N3. *The Plant Cell*. **22**, 3864–3876 (2010).

3. M. Cohn, R. S. Bart, M. Shybut, D. Dahlbeck, M. Gomez, R. Morbitzer, B.-H. Hou, W. B. Frommer, T. Lahaye, B. J. Staskawicz, Xanthomonas axonopodis virulence is promoted by a transcription activator-like effector-mediated induction of a SWEET sugar transporter in cassava. *Mol. Plant Microbe Interact.* **27**, 1186–1198 (2014).

4. Y. Hu, J. Zhang, H. Jia, D. Sosso, T. Li, W. B. Frommer, B. Yang, F. F. White, N. Wang, J. B. Jones, Lateral organ boundaries 1 is a disease susceptibility gene for citrus bacterial canker disease. *PNAS*. **111**, E521–E529 (2014).

5. K. L. Cox, F. Meng, K. E. Wilkins, F. Li, P. Wang, N. J. Booher, S. C. D. Carpenter, L.-Q. Chen, H. Zheng, X. Gao, Y. Zheng, Z. Fei, J. Z. Yu, T. Isakeit, T. Wheeler, W. B. Frommer, P. He, A. J. Bogdanove, L. Shan, TAL effector driven induction of a SWEET gene confers susceptibility to bacterial blight of cotton. *Nature Communications*. **8**, 1–14 (2017).

6. A. Z. Phillips, J. C. Berry, M. C. Wilson, A. Vijayaraghavan, J. Burke, J. I. Bunn, T. W. Allen, T. Wheeler, R. S. Bart, Genomics-enabled analysis of the emergent disease cotton bacterial blight. *PLOS Genetics*. **13**, e1007003 (2017).

7. V. Nekrasov, C. Wang, J. Win, C. Lanz, D. Weigel, S. Kamoun, Rapid generation of a transgene-free powdery mildew resistant tomato by genome deletion. *Sci Rep*. **7**, 482 (2017).

8. A. Peng, S. Chen, T. Lei, L. Xu, Y. He, L. Wu, L. Yao, X. Zou, Engineering canker-resistant plants through CRISPR/Cas9-targeted editing of the susceptibility gene CsLOB1 promoter in citrus. *Plant Biotechnol. J.* **15**, 1509–1519 (2017).

9. Y. Zhang, Y. Bai, G. Wu, S. Zou, Y. Chen, C. Gao, D. Tang, Simultaneous modification of three homoeologs of TaEDR1 by genome editing enhances powdery mildew resistance in wheat. *The Plant Journal*. **91**, 714–724 (2017).

10. M. A. Gomez, Z. D. Lin, T. Moll, R. D. Chauhan, L. Hayden, K. Renninger, G. Beyene, N. J. Taylor, J. C. Carrington, B. J. Staskawicz, R. S. Bart, Simultaneous CRISPR/Cas9-mediated editing of cassava eIF4E isoforms nCBP-1 and nCBP-2 reduces cassava brown streak disease symptom severity and incidence. *Plant Biotechnol. J.* **17**, 421–434 (2019).

11. Z. Xu, X. Xu, Q. Gong, Z. Li, Y. Li, S. Wang, Y. Yang, W. Ma, L. Liu, B. Zhu, L. Zou, G. Chen, Engineering Broad-Spectrum Bacterial Blight Resistance by Simultaneously Disrupting Variable TALE-Binding Elements of Multiple Susceptibility Genes in Rice. *Molecular Plant*. **12**, 1434–1446 (2019).

12. Z. Chu, M. Yuan, J. Yao, X. Ge, B. Yuan, C. Xu, X. Li, B. Fu, Z. Li, J. L. Bennetzen, Q. Zhang, S. Wang, Promoter mutations of an essential gene for pollen development result in disease resistance in rice. *Genes Dev.* **20**, 1250–1255 (2006).

13. B. Yang, A. Sugio, F. F. White, Os8N3 is a host disease-susceptibility gene for bacterial blight of rice. *PNAS*. **103**, 10503–10508 (2006).

14. R. Oliva, C. Ji, G. Atienza-Grande, J. C. Huguet-Tapia, A. Perez-Quintero, T. Li, J.-S. Eom, C. Li, H. Nguyen, B. Liu, F. Auguy, C. Sciallano, V. T. Luu, G. S. Dossa, S. Cunnac, S. M. Schmidt, I. H. Slamet-Loedin, C. Vera Cruz, B. Szurek, W. B. Frommer, F. F. White, B. Yang, Broad-spectrum resistance to bacterial blight in rice using genome editing. *Nature Biotechnology*. **37**, 1344–1350 (2019).

15. S. Bultmann, R. Morbitzer, C. S. Schmidt, K. Thanisch, F. Spada, J. Elsaesser, T. Lahaye, H. Leonhardt, Targeted transcriptional activation of silent oct4 pluripotency gene by combining designer TALEs and inhibition of epigenetic modifiers. *Nucleic Acids Res*. **40**, 5368–5377 (2012).

16. J. Valton, A. Dupuy, F. Daboussi, S. Thomas, A. Maréchal, R. Macmaster, K. Melliand, A. Juillerat, P. Duchateau, Overcoming Transcription Activator-like Effector (TALE) DNA Binding Domain Sensitivity to Cytosine Methylation*♦. *Journal of Biological Chemistry*. **287**, 38427–38432 (2012).

17. R. C. O'Malley, S. C. Huang, L. Song, M. G. Lewsey, A. Bartlett, J. R. Nery, M. Galli, A. Gallavotti, J. R. Ecker, Cistrome and Epicistrome Features Shape the Regulatory DNA Landscape. *Cell*. **165**, 1280–1292 (2016).

18. J. A. Law, S. E. Jacobsen, Establishing, maintaining and modifying DNA methylation patterns in plants and animals. *Nat Rev Genet*. **11**, 204–220 (2010).

19. H. Zhang, Z. Lang, J.-K. Zhu, Dynamics and function of DNA methylation in plants. *Nat Rev Mol Cell Biol*. **19**, 489–506 (2018).

20. A. Papikian, W. Liu, J. Gallego-Bartolomé, S. E. Jacobsen, Site-specific manipulation of Arabidopsis loci using CRISPR-Cas9 SunTag systems. *Nature Communications*. **10**, 1–11 (2019).

21. B. Ghoshal, C. L. Picard, B. Vong, S. Feng, S. E. Jacobsen, CRISPR-based targeting of DNA methylation in Arabidopsis thaliana by a bacterial CG-specific DNA methyltransferase. *PNAS*. **118** (2021), doi:10.1073/pnas.2125016118.

22. L. M. Johnson, J. Du, C. J. Hale, S. Bischof, S. Feng, R. K. Chodavarapu, X. Zhong, G. Marson, M. Pellegrini, D. J. Segal, D. J. Patel, S. E. Jacobsen, SRA- and SET-domain-containing proteins link RNA polymerase V occupancy to DNA methylation. *Nature*. **507**, 124–128 (2014).

23. J. Gallego-Bartolomé, W. Liu, P. H. Kuo, S. Feng, B. Ghoshal, J. Gardiner, J. M.-C. Zhao, S. Y. Park, J. Chory, S. E. Jacobsen, Co-targeting RNA Polymerases IV and V Promotes Efficient De Novo DNA Methylation in Arabidopsis. *Cell*. **176**, 1068-1082.e19 (2019).

24. E. C. Constantin, I. Cleenwerck, M. Maes, S. Baeyen, C. V. Malderghem, P. D. Vos, B. Cottyn, Genetic characterization of strains named as Xanthomonas axonopodis pv. dieffenbachiae leads to a taxonomic revision of the X. axonopodis species complex. *Plant Pathology*. **65**, 792–806 (2016).

25. C. E. López, A. J. Bernal, Cassava Bacterial Blight: Using Genomics for the Elucidation and Management of an Old Problem. *Tropical Plant Biology*. **5**, 117–126 (2012).

26. Z. J. D. Lin, N. J. Taylor, R. Bart, Engineering Disease-Resistant Cassava. *Cold Spring Harb Perspect Biol*. **11**, a034595 (2019).

27. R. Bart, M. Cohn, A. Kassen, E. J. McCallum, M. Shybut, A. Petriello, K. Krasileva, D. Dahlbeck, C. Medina, T. Alicai, L. Kumar, L. M. Moreira, J. R. Neto, V. Verdier, M. A. Santana, N. Kositcharoenkul, H. Vanderschuren, W. Gruissem, A. Bernal, B. J. Staskawicz, High-throughput genomic sequencing of cassava bacterial blight strains identifies conserved effectors to target for durable resistance. *PNAS*. **109**, E1972–E1979 (2012).

28. M. Cohn, R. Morbitzer, T. Lahaye, B. J. Staskawicz, Comparison of gene activation by two TAL effectors from Xanthomonas axonopodis pv. manihotis reveals candidate host susceptibility genes in cassava. *Mol. Plant Pathol.* **17**, 875–889 (2016).

29. H. Wang, G. Beyene, J. Zhai, S. Feng, N. Fahlgren, N. J. Taylor, R. Bart, J. C. Carrington, S. E. Jacobsen, I. Ausin, CG gene body DNA methylation changes and evolution of duplicated genes in cassava. *PNAS*. **112**, 13729–13734 (2015).

30. K. Aung, Y. Jiang, S. Y. He, The role of water in plant-microbe interactions. *Plant J*. **93**, 771–780 (2018).

31. J. A. Law, I. Ausin, L. M. Johnson, A. A. Vashisht, J.-K. Zhu, J. A. Wohlschlegel, S. E. Jacobsen, A Protein Complex Required for Polymerase V Transcripts and RNA- Directed DNA Methylation in Arabidopsis. *Current Biology*. **20**, 951–956 (2010).

32. N. Taylor, E. Gaitán-Solís, T. Moll, B. Trauterman, T. Jones, A. Pranjal, C. Trembley, V. Abernathy, D. Corbin, C. M. Fauquet, A High-throughput Platform for the Production and Analysis of Transgenic Cassava (Manihot esculenta) Plants. *Tropical Plant Biol.* **5**, 127–139 (2012).

33. I. Moreno, W. Gruissem, H. Vanderschuren, Reference genes for reliable potyvirus quantitation in cassava and analysis of Cassava brown streak virus load in host varieties. *Journal of Virological Methods*. **177**, 49–54 (2011).

34. M. Hu, W. Hu, Z. Xia, X. Zhou, W. Wang, Validation of Reference Genes for Relative Quantitative Gene Expression Studies in Cassava (Manihot esculenta Crantz) by Using Quantitative Real-Time PCR. *Front. Plant Sci.* **7** (2016), doi:10.3389/fpls.2016.00680.

35. J. Hellemans, G. Mortier, A. De Paepe, F. Speleman, J. Vandesompele, qBase relative quantification framework and software for management and automated analysis of real-time quantitative PCR data. *Genome Biology*. **8**, R19 (2007).

36. J. Schindelin, I. Arganda-Carreras, E. Frise, V. Kaynig, M. Longair, T. Pietzsch, S. Preibisch, C. Rueden, S. Saalfeld, B. Schmid, J.-Y. Tinevez, D. J. White, V. Hartenstein, K. Eliceiri, P. Tomancak, A. Cardona, Fiji: an open-source platform for biological-image analysis. *Nat Methods*. **9**, 676–682 (2012).

37. G. Beyene, R. D. Chauhan, J. Gehan, D. Siritunga, N. Taylor, Cassava shrunken-2 homolog MeAPL3 determines storage root starch and dry matter content and modulates storage root postharvest physiological deterioration. *Plant Mol Biol* (2020), doi:10.1007/s11103-020-00995-z.

Acknowledgments: We are grateful to our scientific advisory board including Drs. Morag Ferguson, Nathan Springer, and Nigel Taylor. We also acknowledge Dr. Noah Fahlgren, Director of the Data Science lab at DDPSC, and the additional members of our labs who contributed to this work in various ways especially Ke Ke, Molly Kuhs, Dr. Xinggou Zheng, and Dr. Daniel Z. Lin. We also thank David Segal for assistance with the design of the artificial zinc finger.

Funding:

Bill and Melinda Gates Foundation OPP1125410 (RBS, SBJ, JCC)

National Science Foundation GRFP DGE-2139839 and DGE-1745038 (KE)

Author contributions:

Conceptualization: SMW, JCC, SEJ, RSB

Methodology: KMV, KE, GJ, ZZ, SF, MY, KBG, JCB, BG, JGB, JCC, SEJ, RSB

Investigation: KMV, KE, GJ, ZZ, SF, MY, KBG, JCB, BG, JGB, JN

Visualization: KMV, KE, ZZ, MY, KBG, JCB

Funding acquisition: SMW, JCC, SEJ, RSB

Project administration: KBG, JN, SMW, JCC, SEJ, RSB

Supervision: SMW, JCC, SEJ, RSB

Writing – original draft: KMV, ZZ, RSB

Writing – review & editing: KMV, KE, GJ, ZZ, SF, MY, KBG, JCB, BG, JGB, JN, SMW, JCC, SEJ, RSB

Competing interests: Authors declare that they have no competing interests.

Data and materials availability: All amplicon-based bisulfite sequencing data, western blots, images used for imaged-based analysis of water-soaking disease symptoms, and R code for generating plots are available in a FigShare repository (DOI: 10.6084/m9.figshare.16887934). Whole genome bisulfite sequencing data is available at GEO:

GSM5667182 - WGBS data of wild type TME419
GSM5667183 - WGBS data of DMS3-ZF line 133
GSM5667184 - WGBS data of DMS3-ZF line 204

Supplementary Materials

Materials and Methods

Figs. S1 to S11

Table S1

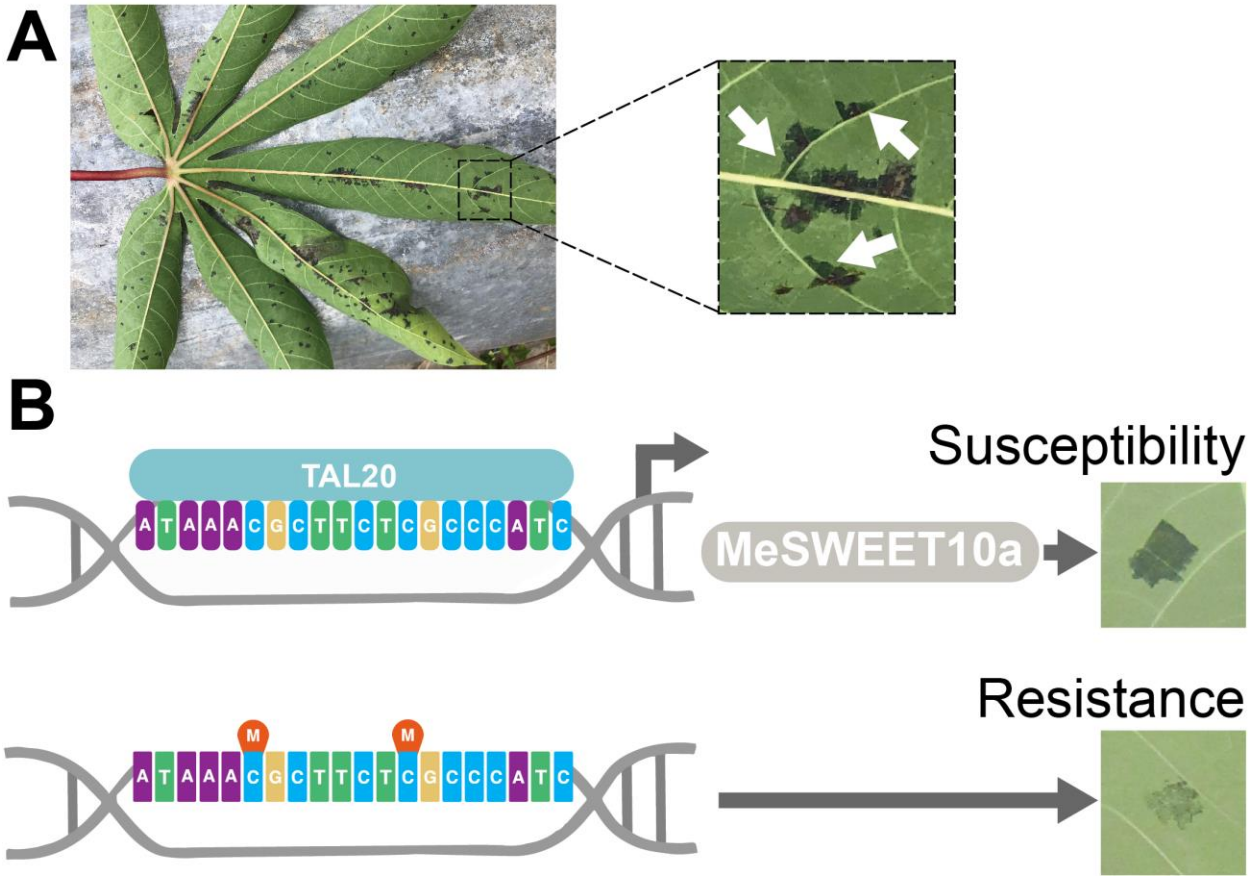

Fig. 1. Overview of strategy to improve disease resistance using epigenetic modification. (**A**) Left: Example of CBB-infected cassava in a field (Uganda, 2019). Right: selected region from leaf on the left. Water-soaked regions are indicated with white arrows. (**B**) Graphical representation of epigenetic CBB disease resistance strategy. Top: In WT plants, TAL20 from *Xam* binds a specific sequence (EBE) present in the promoter of the S gene *MeSWEET10a*. Upon binding, TAL20 induces the ectopic expression of MeSWEET10a, a sugar transporter, which is required for establishment of disease. A typical 'water-soaked' lesion is shown to the right, an early indicator of CBB. Bottom: DNA methylation at two CpG sites prevents TAL20 from binding the EBE. MeSWEET10a expression is not induced and disease symptoms are reduced.

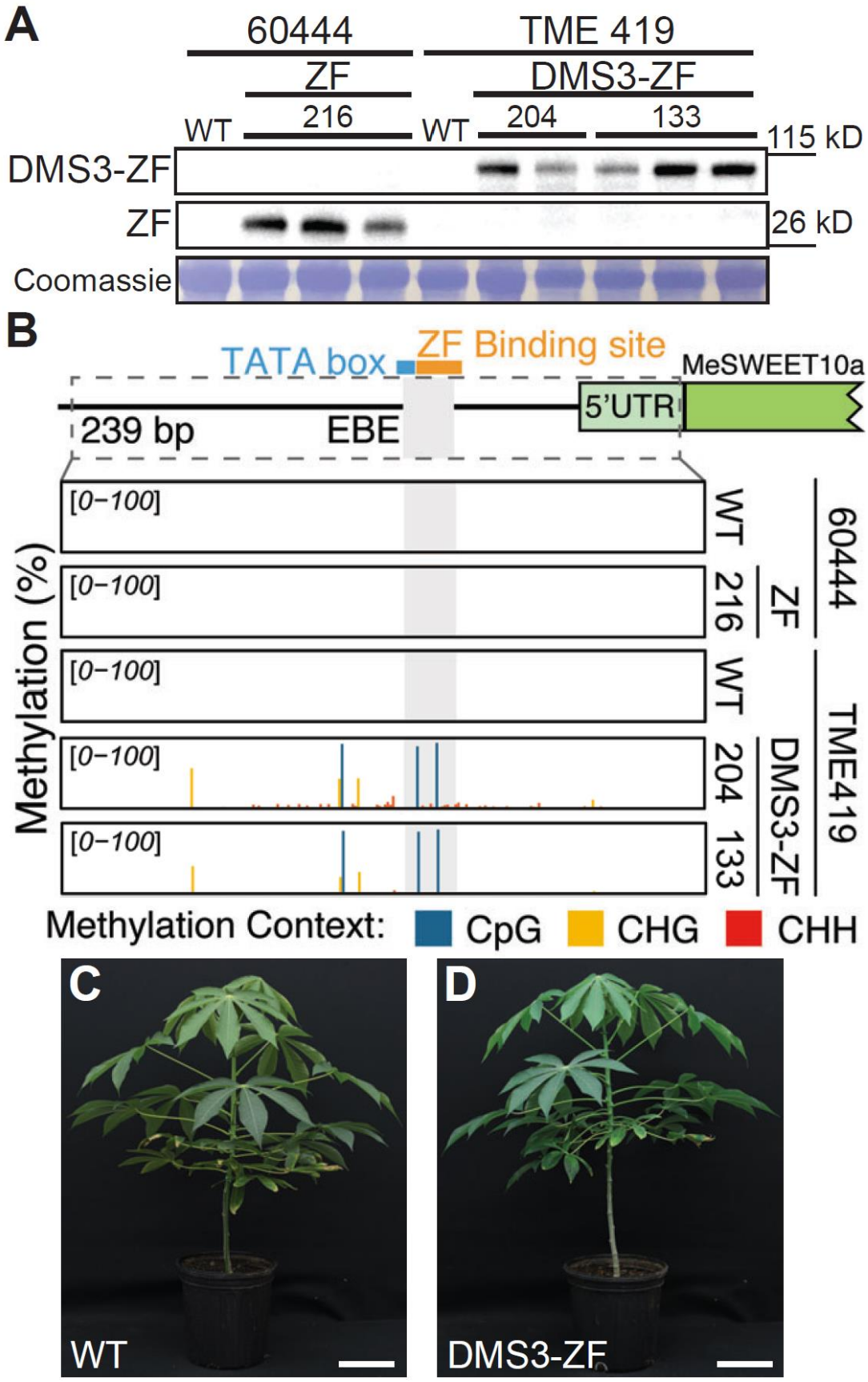
A
60444
TME 419
ZF
DMS3-ZF
WT
216
WT
204
133
115 kD
DMS3-ZF
ZF
26 kD
Coomassie
B
TATA box
ZF Binding site
MeSWEET10a
5'UTR
239 bp
EBE
Methylation (%)
[0–100]
WT
216
ZF
60444
WT
204
133
DMS3-ZF
TME419
Methylation Context:
CpG
CHG
CHH
C
WT
D
DMS3-ZF

295

Fig. 2. DMS3-ZF expression results in CpG methylation at the EBE *in vivo*. (**A**) Expression of transgenes in individual plants from two independent DMS3-expressing transgenic lines (133 and 204) as well as a ZF-only negative control line (216). Cassava variety information for each sample is given above the lanes. First two rows: representative western blots (anti-FLAG) showing expression of the ZF (ZF-3xFLAG) protein with (top) and without (middle) DMS3. Relevant size standards are shown to the right (kD). Bottom: Coomassie Brilliant Blue stained Rubisco, loading control. (**B**) Representative PCR-based bisulfite sequencing (ampBS-seq) results from samples shown in A. Top: Graphical depiction of *MeSWEET10a* promoter region assessed for methylation. The EBE (grey), a presumed TATA box (blue), and the ZF binding site (orange) are indicated. The area within the dotted lined box (239 bp) was subjected to ampBS-seq. Bottom: CpG, CHG, and CHH DNA methylation levels (percent, y-axis) of the *MeSWEET10a* promoter (EBE, grey) measured by ampBS-seq with and without DMS3-ZF. Background of tissue for each plot is indicated to the right. (**C**) Representative wild-type (TME419) and (**D**) DMS3-ZF-expressing (line #133) plants. Scale bar = 14 cm. Additional data quantifying growth in the field are shown in **Fig. S8**.

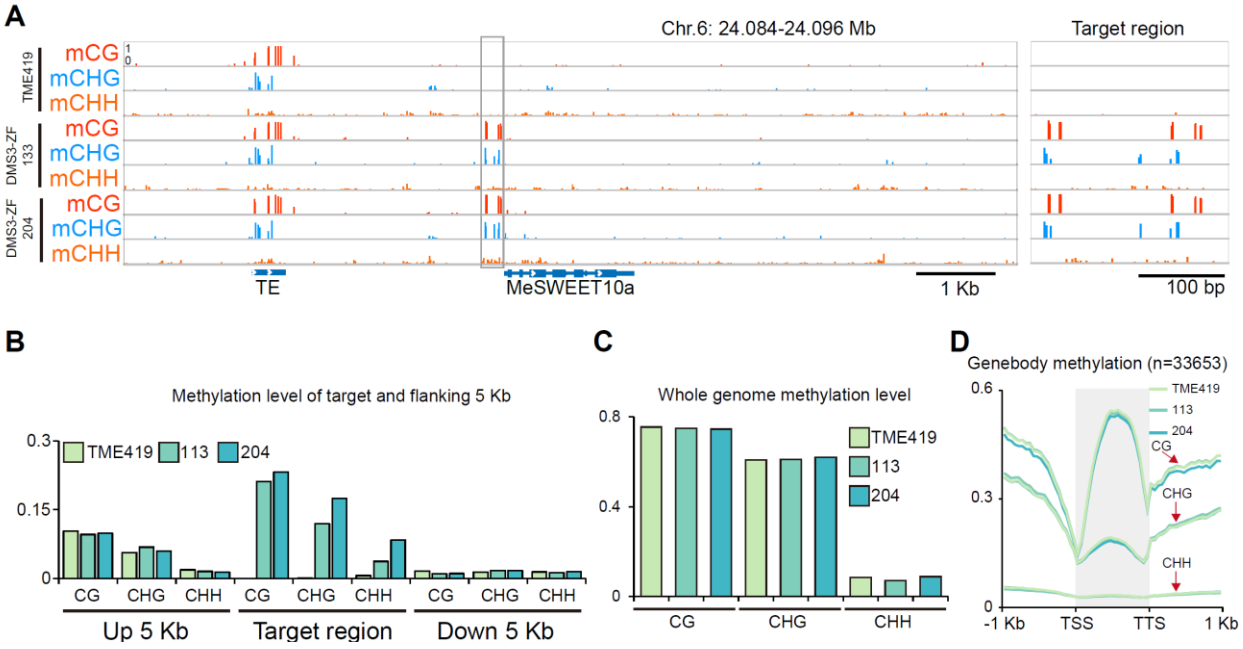

Fig. 3. Targeted methylation at MeSWEET10a shows high specificity. (A) Distribution of CpG, CHG, and CHH methylation over the targeted and flanking 5 kb regions of the *MeSWEET10a* promoter in wild-type TME419 and two independent DMS3-ZF lines (transgenic lines 133 and 204). Grey box indicates the targeted region within the *MeSWEET10a* promoter. **(B)** Summary of CpG, CHG, and CHH methylation level of targeted and flanking 5 kb regions of the *MeSWEET10a* promoter in wild-type TME419 and the two independent DMS3-ZF lines. **(C)** Whole genome CpG, CHG, and CHH methylation level of wild-type TME419 and the two representative DMS3-ZF lines. **(D)** Metaplot of CpG, CHG, and CHH methylation over the gene of protein coding genes (n=33,653) and flanking 1 kb regions in wild-type TME419 and the two independent DMS3-ZF lines.

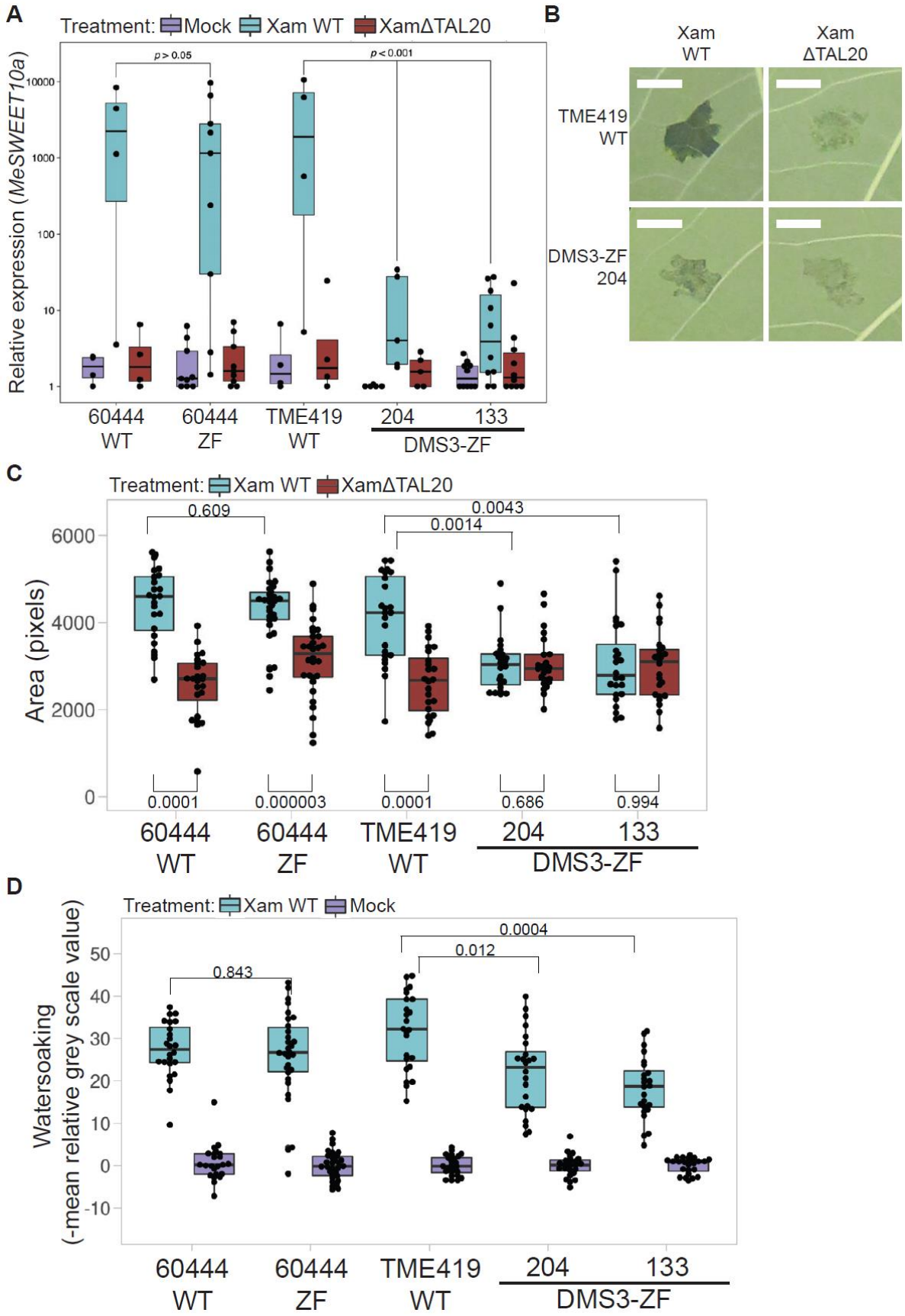
A
Treatment: Mock Xam WT XamΔTAL20
Relative expression (MeSWEET10a)
p > 0.05
p < 0.001
60444 WT
60444 ZF
TME419 WT
204
133
DMS3-ZF
B
Xam WT
Xam ΔTAL20
TME419 WT
DMS3-ZF 204
C
Treatment: Xam WT XamΔTAL20
Area (pixels)
0.609
0.0043
0.0014
0.0001
0.000003
0.0001
0.686
0.994
60444 WT
60444 ZF
TME419 WT
204
133
DMS3-ZF
D
Treatment: Xam WT Mock
Watersoaking (-mean relative grey scale value)
0.843
0.0004
0.012
60444 WT
60444 ZF
TME419 WT
204
133
DMS3-ZF

324

Fig. 4. Effect of methylation on CBB disease phenotypes in cassava. (**A**) Normalized *MeSWEET10a* expression (y-axis, Log10 scale) in WT and transgenic lines as determined by RT-qPCR. The cassava genes GTPb (Manes.09G086600) and PP2A4 (Manes.09G039900) were used as internal controls. Boxes are colored according to Xanthomonas treatment. Biological replicates (black dots) included in each background (x-axis) are as follows: n = 4, 9, 4, 5, 10. Horizontal black line within boxes indicates the value of the median while the box limits indicate the 25th and 75th percentiles as determined by R software; whiskers extend 1.5 times the interquartile range (1.5xIQR) from the 25th and 75th percentiles. Welch's *t*-test *p*-values are noted above brackets within plot. (**B**) Representative images of water-soaking phenotype of leaves from TME419 WT and DMS3-ZF-expressing plants. Images were taken 4 days post-infection with either *Xam668* (XamWT) or a *Xam668* TAL20 deletion mutant (XamΔTAL20). Scale bar = 0.5 cm. (**C**) Observed area (pixels, y-axis) of water-soaking from images of Xam-infiltrated leaves (backgrounds, x-axis) 4 days post-infiltration. Images from (**B**) and **Fig. S11** are included in dataset. Calculated *p*-values (Kolmogorov-Smirnov test) are shown above brackets within plot. (**D**) Intensity of water-soaking phenotype (y-axis) of region measured in panel **C**. The negative mean grey-scale value for the water-soaked region relative to a mock-treated sample within the same leaf is reported. Calculated *p* values (Kolmogorov-Smirnov test) are shown above brackets within plot. Both box plots: Biological replicate values are indicated by dots. Horizontal black line within boxes indicates the value of the median while the box limits indicate the 25th and 75th percentiles as determined by R software; whiskers extend 1.5 times the interquartile range (1.5xIQR) from the 25th and 75th percentiles.

Supplementary Materials for

Improving disease resistance in plants by editing the epigenome

Kira M. Veley, Kiona Elliott, Greg Jensen, Zhenhui Zhong, Suhua Feng, Marisa Yoder, Kerrigan B. Gilbert, Jeffrey C. Berry, Basudev Ghoshal, Javier Gallego-Bartolomé, Joanna Norton, Sharon Motomura-Wages, James C. Carrington, Steven E. Jacobsen, Rebecca S. Bart

Correspondence to: jacobsen@ucla.edu and rbart@danforthcenter.org

This PDF file includes:

Materials and Methods
Figs. S1 to S11
Table S1

Other Supplementary Materials for this manuscript include the following:

All amplicon-based bisulfite sequencing (ampBS-seq) data, western blots, images used for imaged-based analysis of water-soaking disease symptoms, and R code for generating plots are available in a FigShare repository (DOI: 10.6084/m9.figshare.16887934)). Whole genome bisulfite sequencing (WGBS) data is available at GEO (GSM5667182, GSM5667183, GSM5667184).

Materials and Methods

Construct design and cloning

The genomic coding sequence of Arabidopsis *DMS3* (AT3G49250), including promoter, was cloned into the pEG302 backbone as described (*23*, *31*). The ZF targeting the EBE of *MeSWEET10a* was designed as previously described (*22*) to target the sequence 5'-CGCTTCTCGCCCATCCAT-3'. Codelt (zinc.genomecenter.ucdavis.edu:8080/Plone/codeit) was used to generate the amino acid in silico (linker type "normal"). The resulting amino acid sequence was plant codon optimized, synthesized by IDT and cloned at the 3' end of *DMS3* (AT3G49250) in pEG302. A hygromycin resistance cassette was cloned into an available PmeI site for selection in cassava. Vector sequences and maps are available in supplementary materials.

Production of plants and growth conditions

The transgenic cassava line expressing the ZF with no methylating factor was generated for a different project, and thus a different background was used: 60444 (ZFΔDMS3) versus TME419 (DMS3-ZF). Transgenic cassava lines of cultivar TME419 and 60444 were generated and maintained *in vitro* as described previously (*32*) with some modifications, as follows: transgenic FEC cells were selected for resistance using hygromycin (20 mg / ml) on spread plates (also containing 125 mg / L cefotaxime). On stage 1, 2, and 3 plates, 20 mg / ml hygromycin was used as well. Growth chamber settings used for tissue culture: 28°C +/- 1°C, 75 $\mu mol \cdot m^{-2} \cdot s^{-1}$ light; 16 hrs light / 8 hrs dark. *In vitro* plantlets were propagated and established in soil on a misting bench with domes. Once established, plants were removed from the misting bench and acclimated to greenhouse conditions (28°C; humidity >50%; 16 hrs light / 8 hrs dark;

1000 W light fixtures supplementing natural light levels below 400 W / m^2). 1000 W light fixtures supplementing natural light levels below 400 W / m^2). For field-grown plants, individuals were first established in the greenhouse (natural light and temperature, 17-28 °C, humidity >50%) for 29 weeks then transitioned outside and planted 3 feet apart (field location 19.640, -155.083).

PCR bisulfite sequencing (ampBS-seq) library preparation and analysis

PCR-based BS-seq (ampBS-seq) of the *MeSWEET10a* promoter was performed as described (*4*). Leaf tissue and DNA extracted using the GenElute™ Plant Genomic DNA Miniprep Kit (Sigma) and sodium bisulfite treated using the Epitect Bisulfite Conversion kit (QIAGEN). The region of interest within the *MeSWEET10a* promoter was amplified using the primers in Table S1, 233bp product. Libraries were generated from purified PCR products amplified from the bisulfite-treated DNA, using an Ovation Ultralow V2 kit (NuGEN) or a Kapa DNA HyperPrep Kit (Roche) in combination with IDT UD barcodes (Illumina). iSeq 100 (Illumina) was used to sequence the libraries. Raw sequencing reads were aligned to the region of interest using the epigenomic analysis plugin for CLC Genomics Workbench 20.0 (QIAGEN). Reads shorter than 125 bp or longer than 152 bp were discarded. Reads were mapped to the following sequence:
ATATTGTTTTTTTTTTTTTTAAAAAAAATAATAAAAGAAATAAGGTTACTGTTACATT
GACATATTTTATTCACTTTAATCATGCATGCAACTTGACTTCATTCCGTTCCCTGGAT
TCCTCCCCTATATAAACGCTTCTCGCCCATCCATCATTGCACAACATAGCTAGAGTTT
CCTCTTGAGAAAGAGAGTTTCCTCTGCATAAGGGAAAGAGAGTTTTTATTATAGTYG
GA. For mapping, the following parameters were used: non-directional, no masking, match score

= 1, mismatch cost = 2, affine gap cost, insertion open cost = 6, insertion extend cost = 1, deletion open cost = 6, deletion extend cost = 1, length fraction = 0.9, similarity fraction = 0.9. Methylation was called for cytosines with greater than 500 reads mapped and the resulting methylation level was plotted using the provided script (MeSWEET10a_07272021-for_publication.0920.R).

Whole Genome Bisulfite sequencing (WGBS) library preparation and analysis

Genomic DNA from samples were end-repaired and ligated with TruSeq LT DNA single adapters (Illumina) using Kapa DNA HyperPrep kit (Roche). Adapter-ligated DNA was converted with EpiTect Bisulfite Conversion Kit (Qiagen). Converted DNA was PCR-amplified by MyTaq polymerase (Bioline) for 12 cycles. Library quality and size were determined by D1000 ScreenTape (Agilent) and libraries were subsequently purified by AMPure XP beads (Beckman Coulter). Library concentrations were measured with Qubit dsDNA Broad-Range Assay kit (ThermoFisher). Libraries were sequenced on NovaSeq 6000 sequencer (Illumina). WGBS reads were mapped to the TME7 phase0 genome with BSMAP (v2.90) allowing 1 mismatch and 1 best hit (-v 1 -w 1) (*5*, *6*). Duplicated reads were removed with SAMtools (v1.3.1) (*7*). Reads with three or more consecutive methylated CHH sites were considered as unconverted reads and removed in the following analysis. Conversion rate was estimated by calculating methylation level of the chloroplast genome. DNA methylation level at each cytosine was calculated by the number of methylated C vs. total C and T account. Methylation levels of each chromosome were determined by calculating CpG, CHG, and CHH level of 100 kb bins. Methylation track files were visualized with Integrative Genomics Viewer (IGV, v3.0) (*8*).

SDS-PAGE gel and western blotting

All individuals used for qPCR and disease assay experiments were checked for construct expression (S3 (qPCR1), S4 (qPCR2), S5 (Water-soaking), S6 (qPCR3), S7 (Water-soaking, qPCR4), S8 (Water-soaking)). Tissue (100 mg) was collected from each individual plant to be used in an experiment in a 1.5 ml microcentrifuge tube and frozen in liquid nitrogen along with four 3mm glass beads. A tissue lyser (TissueLyser II, QIAGEN) was used to homogenize the sample (30/second frequency, 2 minutes, performed twice with sample rotation between runs). 400 ul of 1x Laemmli Sample buffer (.0625M Tris-HCl pH 6.8, 2% SDS, 10% glycerol, 100 mM DTT) was added to each sample, then samples were boiled 90-100°C for 4 min, centrifuged for 2 min and then either run immediately on a gel or frozen for storage at -80°C. For SDS-PAGE, 10ul of each sample was run on a 12% TEO-Tricine Precast Gel (RunBlue™, AbCam, ab119203) then transferred to PVDF membrane (ThermoFisher Scientific). For western blotting, monoclonal ANTI-FLAG® M2-Peroxidase (HRP) antibody (A8592, Sigma) was used (1:2000 dilution in 5% milk in TBST). HRP activity was assessed using SuperSignal™ West Femto substrate (ThermoFisher Scientific). Chemiluminescence was detected using the ChemiDoc XRS+ System equipped with Image Lab 6.1 software (Bio-Rad). The molecular weight of protein bands was estimated by comparison with the BenchMark™ Pre-stained Protein Ladder (Thermo Fisher Scientific). The abundance of the 3xFLAG-ZF proteins were quantified from the band intensities also using Image Lab Software. Coomassie staining was performed on membranes using Coomassie brilliant blue (0.025% (w/v) Coomassie brilliant blue R-250 (ThermoFisher Scientific) in 40% methanol/7% acetic acid (v/v)). Staining was performed for 3 min followed by destain (solution: 50% methanol/7% acetic acid (v/v)) for 30 min. Then membranes were rinsed with water and allowed to dry overnight before imaging.

Electrophoretic mobility shift assay (EMSA)

For protein purification, *TAL20$_{Xam668}$* was cloned into pDEST17 (Thermo Fisher Scientific) using Gateway™ technology, resulting in the addition of a 6xHis-tag at the N-terminus of the protein upon expression. 6xHis-TAL20$_{Xam668}$ was expressed and purified from *E. coli* BL21 cells using HisPur™ Ni-NTA Spin Columns (Thermo Fisher Scientific). Protein size and purity was assessed by SDS-PAGE (4-12% gradient gel) followed by western blot (Figure S1A) using an anti-His antibody (His-Tag (27E8) Mouse mAb (HRP Conjugate), Cell Signaling Technology). For the EMSA, the sequence previously shown to be able to be bound by TAL20$_{Xam668}$ (*3*), with and without methylation, was synthesized (Integrated DNA Technologies) and biotin-labeled (Pierce™ Biotin 3' End DNA Labeling Kit, Thermo Fisher Scientific). The sequence used is as follows, with methylated cytosines indicated by underlining: sense 5'-CCCTATATAAACGCTTCTCGCCCATCCATCATT-3', anti-sense: 3'-GGGATATATTTGCGAAGAGCGGGTAGGTAGTAA-5'. EMSA was performed with the Light Shift® Chemiluminescent EMSA Kit (Thermo Fisher Scientific) according to the manufacturer's protocol. Biotin-labeled oligonucleotides were mixed with 0, 20, 200, 300 and 1000 fmol of purified TAL20$_{Xam668}$ effector protein as indicated in the chart in Figure S1B. All binding reactions were incubated at room temperature for 20 min. For competition assays, unlabeled oligonucleotides were pre-incubated with other reaction components for an additional 20 min. Gel electrophoresis was performed on a 6% native polyacrylamide gel.

Bacterial inoculations

Xanthomonas strains were grown on plates containing necessary antibiotics for 2-3 days at 30°C. The *Xanthomonas* strains used and their antibiotic resistances are as follows: 1. *Xam668* (rifampicin 50 µg / ml) and 2. *Xam668ΔTAL20* (suicide vector knockout (*3*), tetracycline 5 µg / ml, rifampicin 50 µg / ml). Bacteria were scraped from the plates into 10 mM $MgCl_2$ to either OD_{600} = 1.0 (RT-qPCR) or OD_{600} = 0.01 (water-soaking) concentrations. Leaves (2-3 weeks after plants were transferred to a greenhouse) were inoculated with a 1.0 ml needleless syringe using one bacterial strain per lobe, three injection points on each of 2-3 leaves. After inoculation, plants were kept under fluorescent light (12 hr day / night light cycle) at 27°C for either 48 hours (RT-qPCR and ampBS-seq) or 4, 6, and 9 days (water-soaking).

RNA extraction and RT–qPCR analysis

For RNA, 48 hours post-infiltration, samples were taken using an 8 mm cork borer at each infiltration site, frozen in liquid nitrogen, ground to a fine powder (3 mm glass beads added to tissue, ground using tissue lyser (TissueLyser II, QIAGEN), 30/second frequency, 2 minutes, performed twice with sample rotation between runs) and total RNA was extracted (Spectrum™ Plant Total RNA Kit, Sigma). Technical replicates were pooled, thus each RNA sample contained three injection sites from one leaf. 1.0 µg DNase-treated RNA was reverse-transcribed to cDNA using SuperScript™ III Reverse Transcriptase (Thermo Fisher Scientific) according to the manufacturer's instructions.

Quantitative reverse transcription PCR (RT-qPCR) was done with SYBR Select Master Mix (Thermo Fisher Scientific) on a CFX384 Touch Real-Time PCR Detection System (Bio-Rad). Primers specific for cassava GTPb (Manes.09G086600) and PP2A4 (Manes.09G039900) genes

were used as the internal controls to calculate relative expression levels (Table S1) (*33*, *34*). Normalized relative expression was calculated using formulas described (*35*).

Water-soaking area and intensity quantification, image analysis

Cassava leaves were infiltrated with either 10 mM $MgCl_2$ alone (mock) or containing *Xanthomonas* (*Xam668* strains with and without TAL20) as described above and imaged using a Canon EOS Rebel T5i camera with a 15-85mm lens at 0-, 4-, 6-, and 9-days post-inoculation. Images were gray balanced using a X-Rite Passport by estimating the saturation of the six gray chips and lowering the brightness accordingly. Gray corrected images were uploaded to FIJI (*36*) and duplicated. In order to define the infected area, visible water-soaking spots were manually outlined on the duplicate image using the pencil tool (color: #ff00b6 and size 2). The outlined images were converted from RGB to LAB and split to obtain the A color channel. The A channel images were thresholded, converted to a mask and the mask for each spot was added to the ROI manager using the analyze particle tool. The ROI masks were applied to the original RGB gray corrected images. In order to define the background color of a given leaf, mock-infiltrated spots (no water-soaking) were added to the ROI manager using an arbitrarily sized rectangle selection tool consistently set to a W=51 and H=61. Area and gray scale mean data were obtained for each infiltrated spot using the FIJI measure tool. Gray balancing using the X-Rite Passport is a coarse adjustment and finer standardization is performed post image processing using statistical methods. Gray value standardization was achieved by estimating the grand mean of all gray values in each image and centering those values to the grand mean of all images by using model residuals. Further, the residuals within each image were re-centered with respect to the mock treatment by subtracting the mean gray value of mock from all other features.

Storage root production and measurements

Storage root production and analysis was conducted with some modification as described (*37*). Briefly, plants were maintained in small, 2 inch pots for 11 weeks in order to induce storage root production. The same greenhouse conditions were used as described above. After 11 weeks, roots were removed from pots, washed to remove soil, and storage roots isolated from the root mass and weighed for fresh weight measurements. For starch content estimation (approximately 80% of storage root weight), the storage roots were peeled, cut into approximately 2 cm cubes, placed into a 50 ml conical tube, and frozen in dry ice and stored at -80°C prior to lyophilization. Samples were lyophilized for two days, then weighed to obtain dry weight.

A

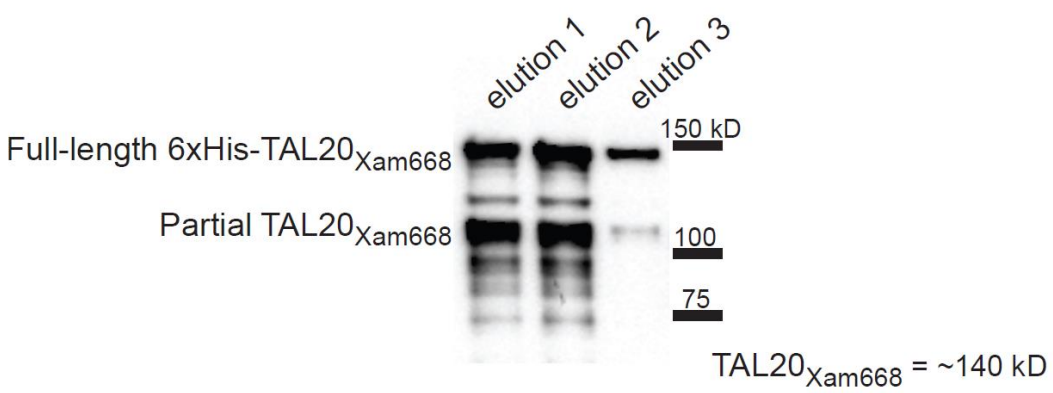

B

EBE sequence:

```
5′ CCCTATATAAACGCTTCTCGCCCATCCATCATT 3′
3′ GGGATATATTTGCGAAGAGCGGGTAGGTAGTAA 5′
```

	Lane 1	2	3	4	5	6	7
$TAL20_{Xam668}$	0	300	300	300	300	300	300 fmol
EBE+Biotin	20	20			20	20	20 fmol
EBE-Biotin					200		
EBEMeth+Biotin			20	200			
EBEMeth−Biotin						200	1000 fmol

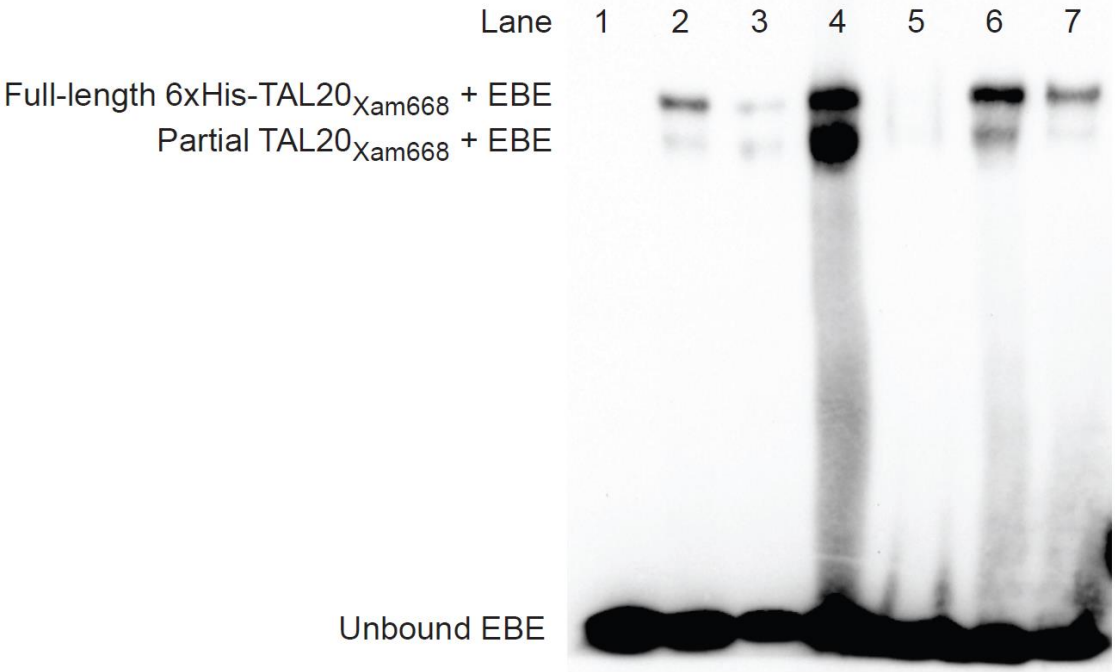

539

Fig. S1. – Binding affinity of TAL20 to EBE is decreased *in vitro* in the presence of methylation.

(**A**) Western blot (anti-His) of elution samples resulting from TAL20 purification from *E. coli*. Three elutions were performed and are shown. Size standards are shown to the right (kD). (**B**) Electrophoretic mobility shift assay (EMSA) between the EBE and His-purified TAL20 (elution 3). The binding reaction components are given in the table with amounts indicated. The DNA sequence used in the binding reactions is shown above the table with the EBE sequence shaded in gray and methylated cytosines indicated in red and underlined. Each reaction corresponds to a lane in the blot shown below. The lower band from the purification, presumed to be partial TAL20 peptide or some other 6xHis-containing product, appears in the EMSA as well, and are labeled as such to the left of the image.

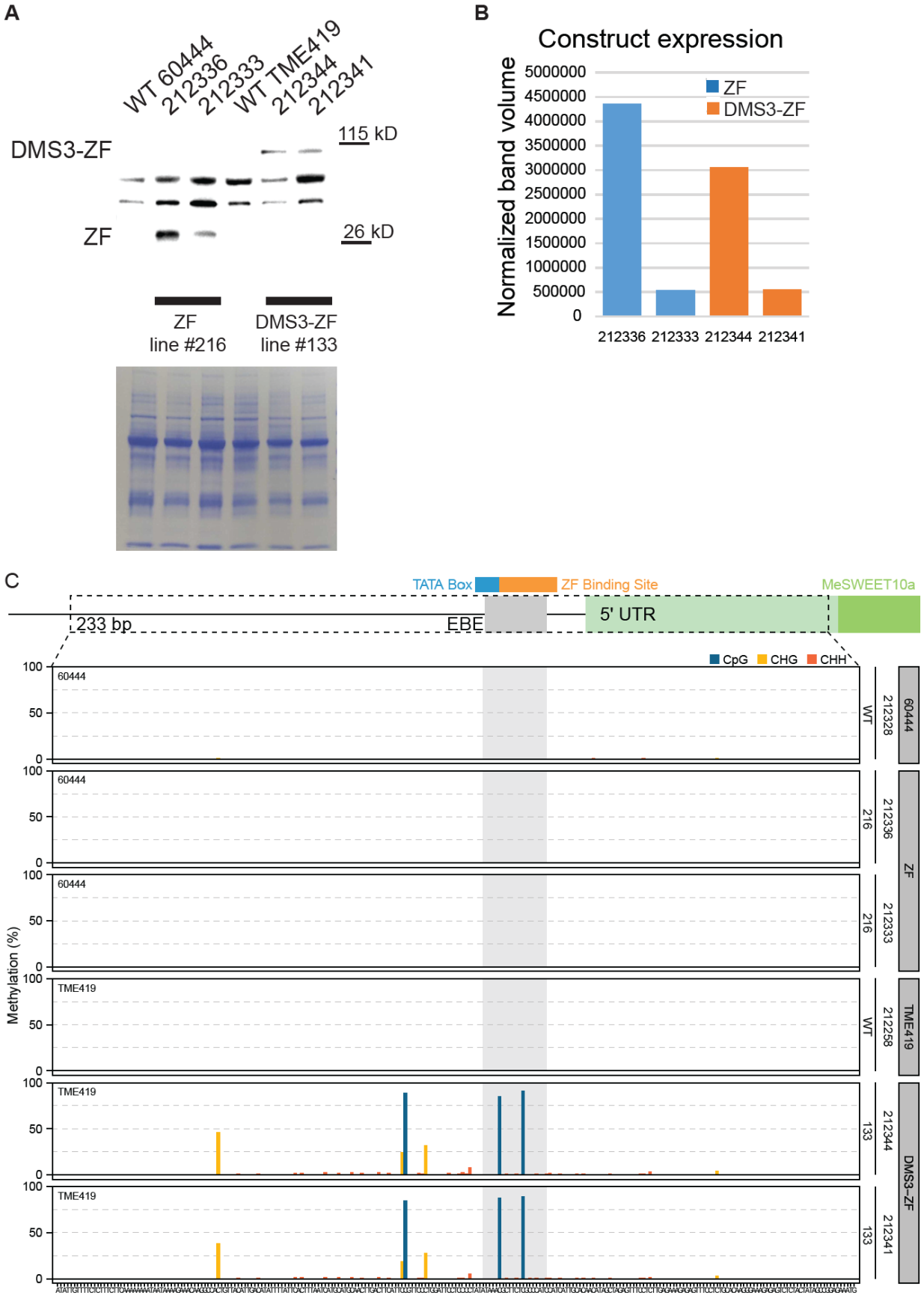
A
WT 60444
212336
212333
WT TME419
212344
212341
DMS3-ZF
115 kD
ZF
26 kD
ZF
line #216
DMS3-ZF
line #133
B
Construct expression
Normalized band volume
5000000
4500000
4000000
3500000
3000000
2500000
2000000
1500000
1000000
500000
0
ZF
DMS3-ZF
212336 212333 212344 212341
C
TATA Box
ZF Binding Site
MeSWEET10a
233 bp
EBE
5' UTR
CpG CHG CHH
Methylation (%)
60444
TME419
WT
216
133
212328
212336
212333
212258
212344
212341
ZF
DMS3-ZF

554

Fig. S2. - Expression and methylation quantification for individuals used in an individual experiment (qPCR1).

(**A**) Expression of transgenes in individual plants from two independent DMS3-expressing transgenic lines (133 and 204) as well as a ZF-only negative control line (216). Top: Western blots (anti-FLAG) showing expression of the ZF (ZF-3xFLAG) protein with and without DMS3. Each individual plant is identified by a number (above each lane) and the necessary wild-type (WT) controls are also included (60444 for ZF and TME 419 for DMS3-ZF lines). Relevant size standards are shown to the right (kD). Bottom: Coomassie Brilliant Blue stained Rubisco, loading control. (**B**) Quantification of the intensity of the bands, expressed as adjusted band volume (relative to Rubisco) according to Image Lab™ software (Bio-Rad). (**C**) PCR bisulfite sequencing (ampBS-seq) results from all samples shown in **A**. Top: Graphical depiction of *MeSWEET10a* promoter region assessed for methylation. The EBE (grey) which overlaps a presumed TATA box (blue), is indicated. The site that the ZF was engineered to bind is shown in orange. The area within the dotted lined box (239 bp) was subjected to ampBS-seq. Bottom: CpG, CHG, and CHH DNA methylation levels (percent, y-axis) of the *MeSWEET10a* promoter (EBE, grey) measured by ampBS-seq with and without DMS3-ZF. Background of tissue for each plot is indicated to the right.

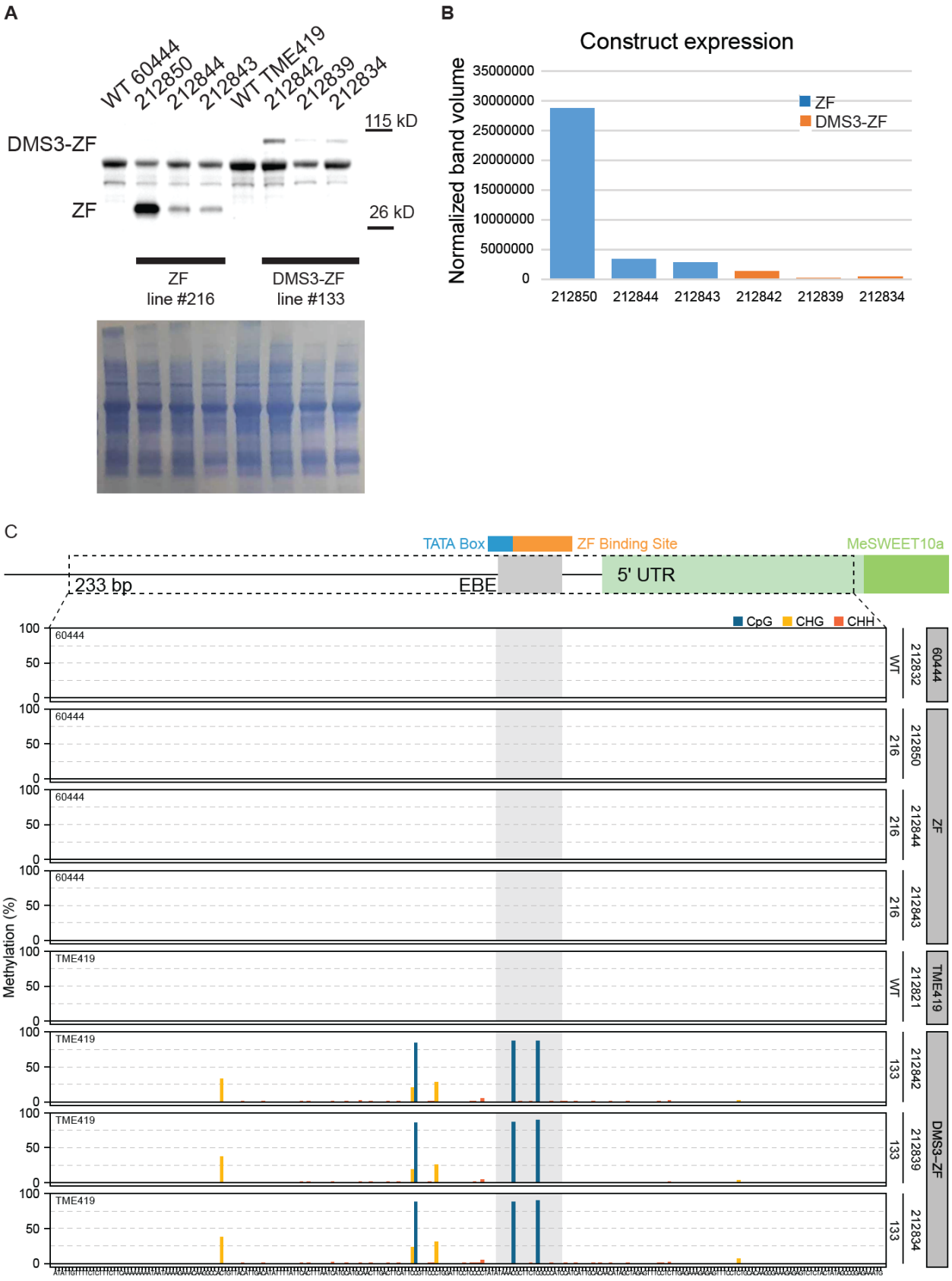
A
WT 60444
212850
212844
212843
WT TME419
212842
212839
212834
115 kD
DMS3-ZF
ZF
26 kD
ZF
line #216
DMS3-ZF
line #133
B
Construct expression
Normalized band volume
35000000
30000000
25000000
20000000
15000000
10000000
5000000
0
ZF
DMS3-ZF
212850
212844
212843
212842
212839
212834
C
TATA Box
ZF Binding Site
MeSWEET10a
233 bp
EBE
5' UTR
CpG
CHG
CHH
Methylation (%)
60444
TME419
WT
216
133
212832
212850
212844
212843
212821
212842
212839
212834
ZF
DMS3-ZF

573

Fig. S3. - Expression and methylation quantification for individuals used in an individual experiment (qPCR2).

(**A**) Expression of transgenes in individual plants from two independent DMS3-expressing transgenic lines (133 and 204) as well as a ZF-only negative control line (216). Top: Western blots (anti-FLAG) showing expression of the ZF (ZF-3xFLAG) protein with and without DMS3. Each individual plant is identified by a number (above each lane) and the necessary wild-type (WT) controls are also included (60444 for ZF and TME 419 for DMS3-ZF lines). Relevant size standards are shown to the right (kD). Bottom: Coomassie Brilliant Blue stained Rubisco, loading control. (**B**) Quantification of the intensity of the bands, expressed as adjusted band volume (relative to Rubisco) according to Image Lab™ software (Bio-Rad). (**C**) PCR bisulfite sequencing (ampBS-seq) results from all samples shown in **A**. Top: Graphical depiction of *MeSWEET10a* promoter region assessed for methylation. The EBE (grey) which overlaps a presumed TATA box (blue), is indicated. The site that the ZF was engineered to bind is shown in orange. The area within the dotted lined box (239 bp) was subjected to ampBS-seq. Bottom: CpG, CHG, and CHH DNA methylation levels (percent, y-axis) of the *MeSWEET10a* promoter (EBE, grey) measured by ampBS-seq with and without DMS3-ZF. Background of tissue for each plot is indicated to the right.

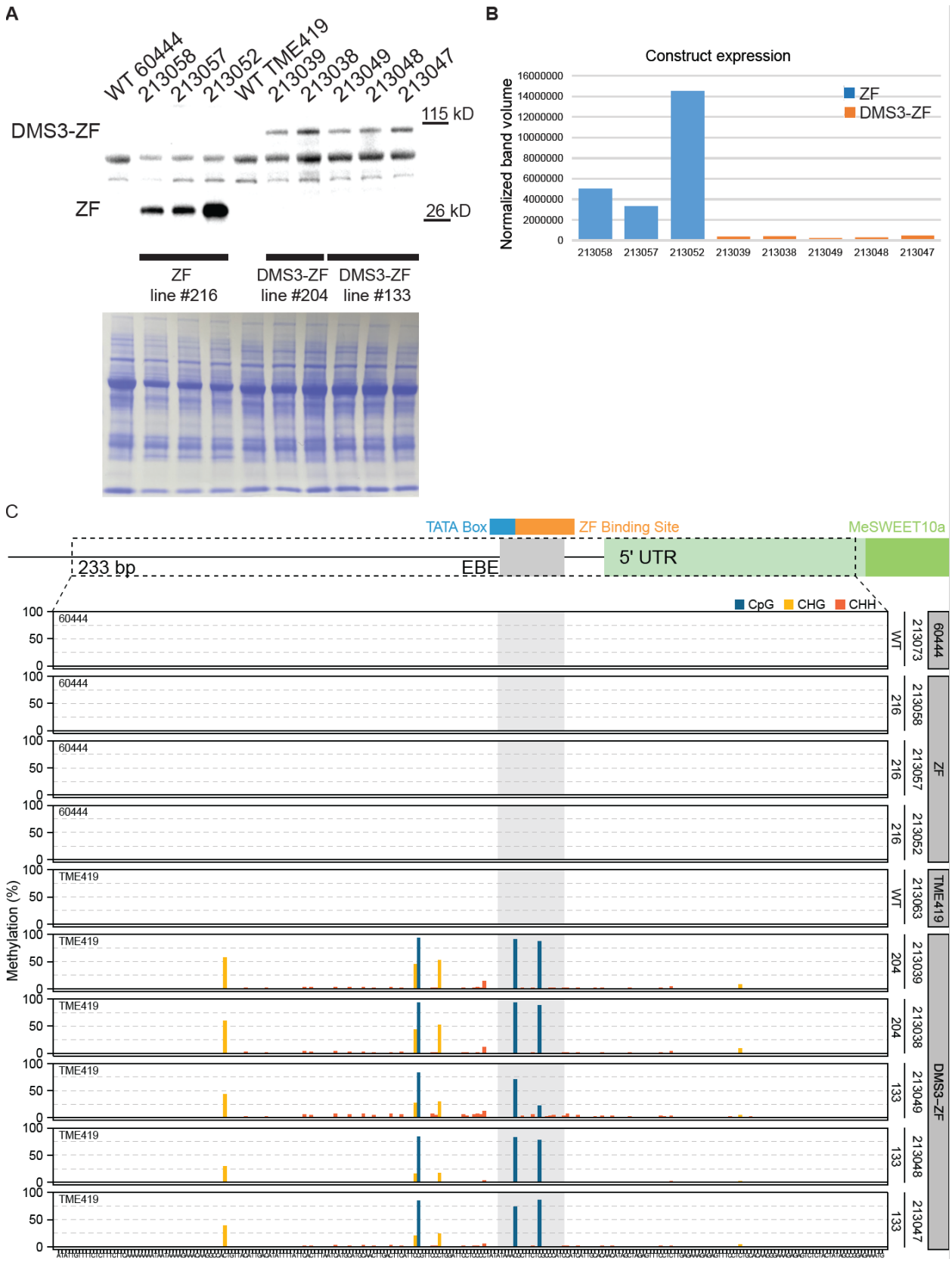
A
WT 60444
213058
213057
213052
WT TME419
213039
213038
213049
213048
213047
DMS3-ZF
ZF
115 kD
26 kD
ZF line #216
DMS3-ZF line #204
DMS3-ZF line #133
B
Construct expression
Normalized band volume
ZF
DMS3-ZF
C
TATA Box
ZF Binding Site
MeSWEET10a
233 bp
EBE
5' UTR
CpG
CHG
CHH
Methylation (%)
60444
TME419
WT
ZF
DMS3-ZF

592

Fig. S4. - Expression and methylation quantification for individuals used in an individual experiment (water-soaking).

(**A**) Expression of transgenes in individual plants from two independent DMS3-expressing transgenic lines (133 and 204) as well as a ZF-only negative control line (216). Top: Western blots (anti-FLAG) showing expression of the ZF (ZF-3xFLAG) protein with and without DMS3. Each individual plant is identified by a number (above each lane) and the necessary wild-type (WT) controls are also included (60444 for ZF and TME 419 for DMS3-ZF lines). Relevant size standards are shown to the right (kD). Bottom: Coomassie Brilliant Blue stained Rubisco, loading control. (**B**) Quantification of the intensity of the bands, expressed as adjusted band volume (relative to Rubisco) according to Image Lab™ software (Bio-Rad). (**C**) PCR bisulfite sequencing (ampBS-seq) results from all samples shown in **A**. Top: Graphical depiction of *MeSWEET10a* promoter region assessed for methylation. The EBE (grey) which overlaps a presumed TATA box (blue), is indicated. The site that the ZF was engineered to bind is shown in orange. The area within the dotted lined box (239 bp) was subjected to ampBS-seq. Bottom: CpG, CHG, and CHH DNA methylation levels (percent, y-axis) of the *MeSWEET10a* promoter (EBE, grey) measured by ampBS-seq with and without DMS3-ZF. Background of tissue for each plot is indicated to the right.

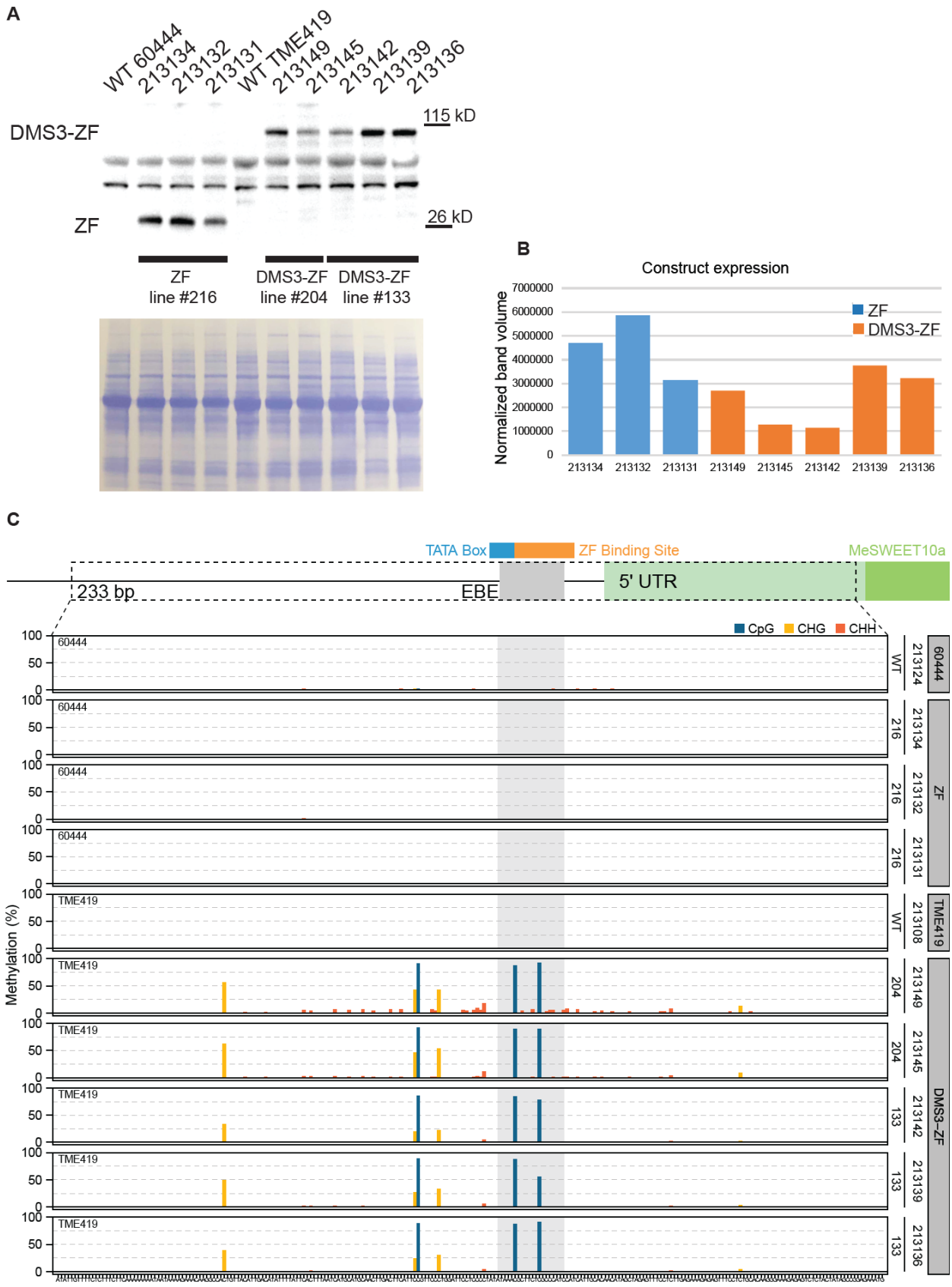
A
WT 60444
213134
213132
213131
WT TME419
213149
213145
213142
213139
213136
DMS3-ZF
115 kD
ZF
26 kD
ZF line #216
DMS3-ZF line #204
DMS3-ZF line #133
B
Construct expression
Normalized band volume
ZF
DMS3-ZF
213134
213132
213131
213149
213145
213142
213139
213136
C
TATA Box
ZF Binding Site
MeSWEET10a
233 bp
EBE
5' UTR
CpG
CHG
CHH
Methylation (%)
60444
TME419
WT
216
204
133
ZF
DMS3-ZF

611

Fig. S5. - Expression and methylation quantification for individuals used in an individual experiment (qPCR3).

(**A**) Expression of transgenes in individual plants from two independent DMS3-expressing transgenic lines (133 and 204) as well as a ZF-only negative control line (216). Top: Western blots (anti-FLAG) showing expression of the ZF (ZF-3xFLAG) protein with and without DMS3. Each individual plant is identified by a number (above each lane) and the necessary wild-type (WT) controls are also included (60444 for ZF and TME 419 for DMS3-ZF lines). Relevant size standards are shown to the right (kD). Bottom: Coomassie Brilliant Blue stained Rubisco, loading control. (**B**) Quantification of the intensity of the bands, expressed as adjusted band volume (relative to Rubisco) according to Image Lab™ software (Bio-Rad). (**C**) PCR bisulfite sequencing (ampBS-seq) results from all samples shown in **A**. Top: Graphical depiction of *MeSWEET10a* promoter region assessed for methylation. The EBE (grey) which overlaps a presumed TATA box (blue), is indicated. The site that the ZF was engineered to bind is shown in orange. The area within the dotted lined box (239 bp) was subjected to ampBS-seq. Bottom: CpG, CHG, and CHH DNA methylation levels (percent, y-axis) of the *MeSWEET10a* promoter (EBE, grey) measured by ampBS-seq with and without DMS3-ZF. Background of tissue for each plot is indicated to the right.

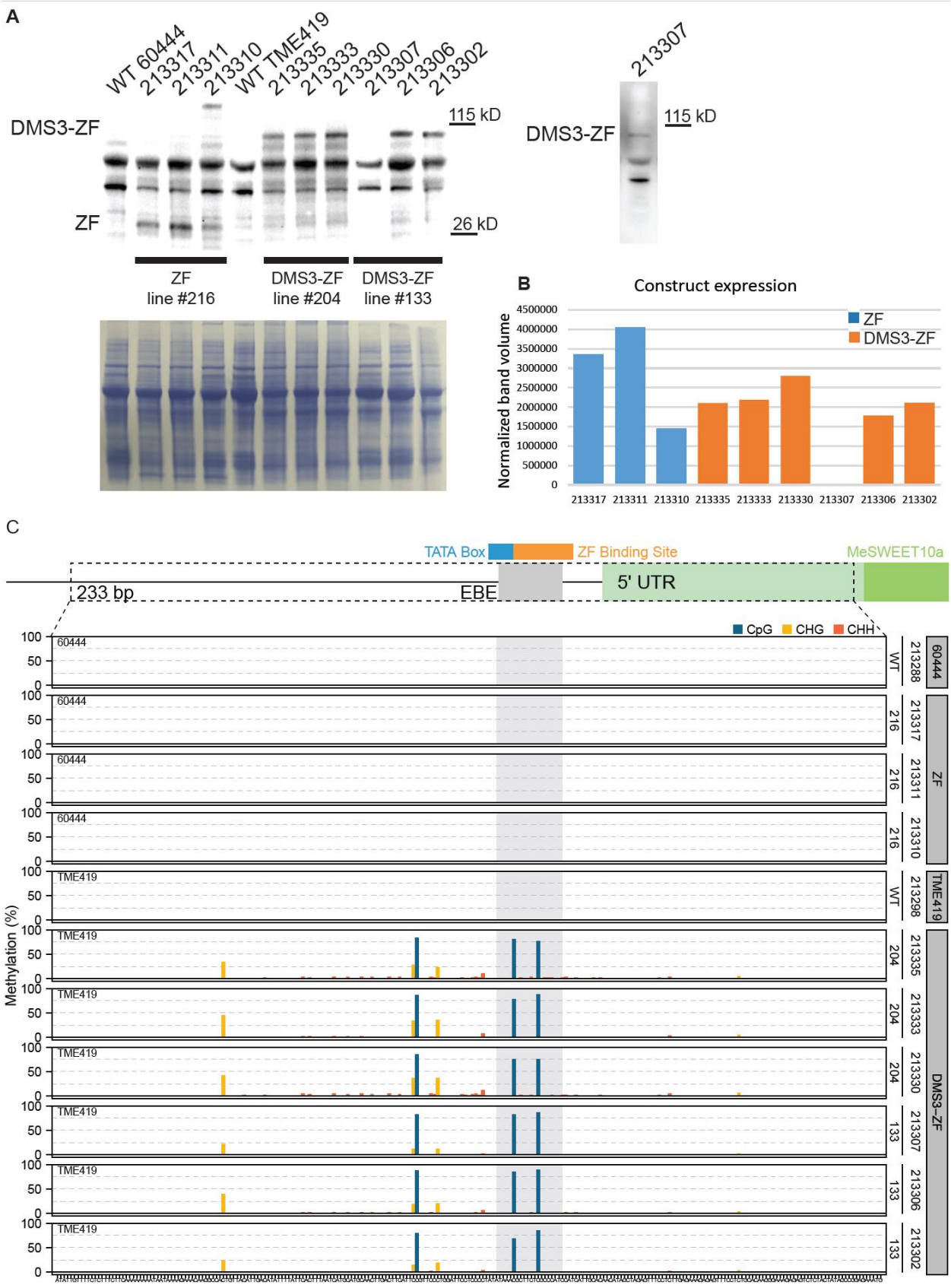
A
WT 60444
213317
213311
213310
WT TME419
213335
213333
213330
213307
213306
213302
DMS3-ZF
ZF
115 kD
26 kD
ZF line #216
DMS3-ZF line #204
DMS3-ZF line #133
213307
DMS3-ZF
115 kD
B
Construct expression
Normalized band volume
ZF
DMS3-ZF
213317 213311 213310 213335 213333 213330 213307 213306 213302
C
TATA Box
ZF Binding Site
MeSWEET10a
233 bp
EBE
5' UTR
CpG CHG CHH
Methylation (%)
60444
TME419
WT
216
204
133
ZF
DMS3-ZF

630

Fig. S6. - Expression and methylation quantification for individuals used as an individual experiment set (qPCR4, water-soaking).

(**A**) Expression of transgenes in individual plants from two independent DMS3-expressing transgenic lines (133 and 204) as well as a ZF-only negative control line (216). Top: Western blots (anti-FLAG) showing expression of the ZF (ZF-3xFLAG) protein with and without DMS3. Each individual plant is identified by a number (above each lane) and the necessary wild-type (WT) controls are also included (60444 for ZF and TME 419 for DMS3-ZF lines). Relevant size standards are shown to the right (kD). Bottom: Coomassie Brilliant Blue stained Rubisco, loading control. Right: Example replicate blot showing expression of DMS3-ZF in individual 213307. No expression of DMS3-ZF was detected in individual 213307 in the blot used for quantification. Additional repeats of western blot analysis on that sample showed evidence of detectable expression of DMS3-ZF. (**B**) Quantification of the intensity of the bands shown in **A**, expressed as adjusted band volume (relative to Rubisco) according to Image Lab™ software (Bio-Rad). (**C**) PCR bisulfite sequencing (ampBS-seq) results from all samples shown in **A**. Top: Graphical depiction of *MeSWEET10a* promoter region assessed for methylation. The EBE (grey) which overlaps a presumed TATA box (blue), is indicated. The site that the ZF was engineered to bind is shown in orange. The area within the dotted lined box (239 bp) was subjected to ampBS-seq. Bottom: CpG, CHG, and CHH DNA methylation levels (percent, y-axis) of the *MeSWEET10a* promoter (EBE, grey) measured by ampBS-seq with and without DMS3-ZF. Background of tissue for each plot is indicated to the right.

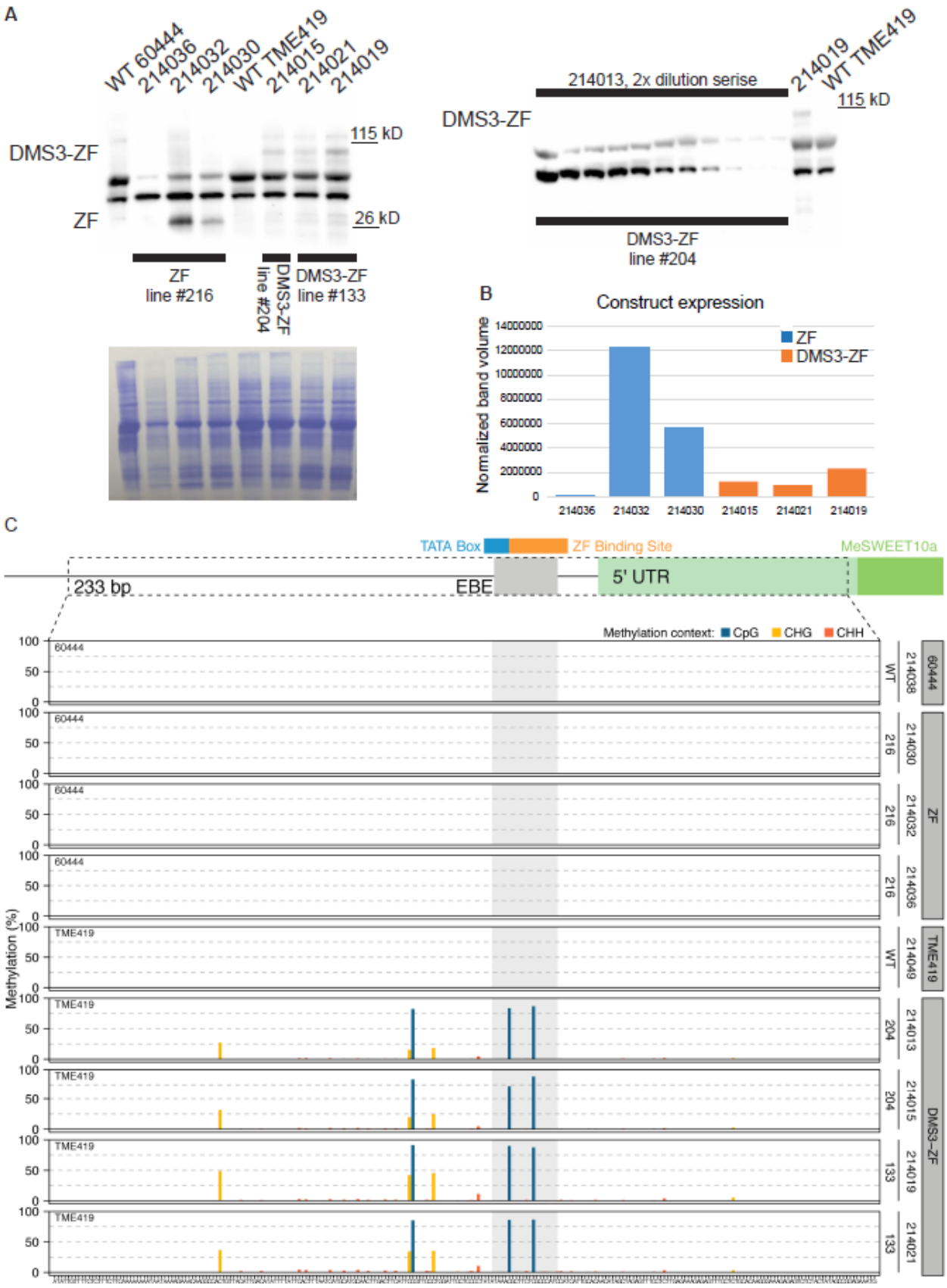
A
WT 60444
214036
214032
214030
WT TME419
214015
214021
214019
DMS3-ZF
ZF
115 kD
26 kD
ZF
line #216
DMS3-ZF
line #204
DMS3-ZF
line #133
214013, 2x dilution serise
214019
WT TME419
115 kD
DMS3-ZF
DMS3-ZF
line #204
B
Construct expression
Normalized band volume
ZF
DMS3-ZF
214036
214032
214030
214015
214021
214019
C
TATA Box
ZF Binding Site
MeSWEET10a
233 bp
EBE
5' UTR
Methylation context: CpG CHG CHH
Methylation (%)
60444
TME419
ZF
DMS3-ZF

652

Fig. S7. - Expression and methylation quantification for individuals used in an individual experiment (water-soaking).

(**A**) Expression of transgenes in individual plants from two independent DMS3-expressing transgenic lines (133 and 204) as well as a ZF-only negative control line (216). Top: Western blots (anti-FLAG) showing expression of the ZF (ZF-3xFLAG) protein with and without DMS3. Each individual plant is identified by a number (above each lane) and the necessary wild-type (WT) controls are also included (60444 for ZF and TME 419 for DMS3-ZF lines). Relevant size standards are shown to the right (kD). Bottom: Coomassie Brilliant Blue stained Rubisco, loading control. Right: Example dilution series blot showing the lack detectible expression of DMS3-ZF in an individual (214013) included in a water-soaking experiment. (**B**) Quantification of the intensity of the bands shown in A, expressed as adjusted band volume (relative to Rubisco) according to Image Lab™ software (Bio-Rad). (**C**) PCR bisulfite sequencing (ampBS-seq) results from all samples shown in **A**. Top: Graphical depiction of *MeSWEET10a* promoter region assessed for methylation. The EBE (grey) which overlaps a presumed TATA box (blue), is indicated. The site that the ZF was engineered to bind is shown in orange. The area within the dotted lined box (239 bp) was subjected to ampBS-seq. Bottom: CpG, CHG, and CHH DNA methylation levels (percent, y-axis) of the *MeSWEET10a* promoter (EBE, grey) measured by ampBS-seq with and without DMS3-ZF. Background of tissue for each plot is indicated to the right. Note: the observed methylation in individual 214013 is indistinguishable from other individuals, despite undetectable expression of the DMS3-ZF construct.

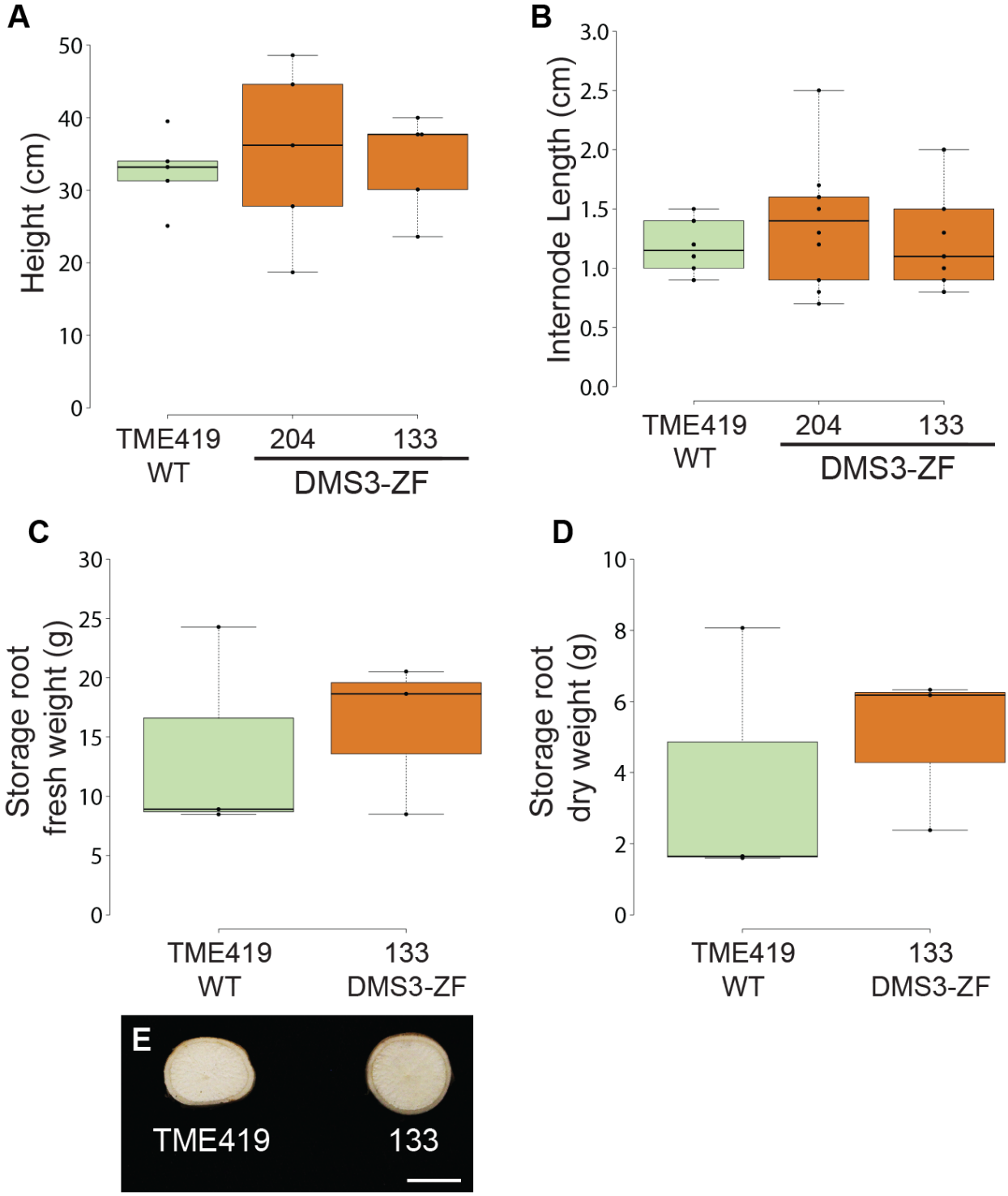
A
Height (cm)
50
40
30
20
10
0
TME419
WT
204
133
DMS3-ZF
B
Internode Length (cm)
3.0
2.5
2.0
1.5
1.0
0.5
0.0
TME419
WT
204
133
DMS3-ZF
C
Storage root
fresh weight (g)
30
25
20
15
10
5
0
TME419
WT
133
DMS3-ZF
D
Storage root
dry weight (g)
10
8
6
4
2
0
TME419
WT
133
DMS3-ZF
E
TME419
133

677

678

679

Fig. S8. – Developmental characteristics are indistinguishable between wild-type and methylated transgenic lines.

(A) Height and **(B)** internode length of individual wild-type (WT, green) and DMS3-ZF (orange), field-grown plants after approximately 6 months in soil. Internode measurements for each plant were taken on the stem just above and below the woody transition. Biological replicate values are indicated by dots. Horizontal black line within boxes indicates the value of the median while the box limits indicate the 25th and 75th percentiles as determined by R software; whiskers extend 1.5 times the interquartile range (1.5xIQR) from the 25th and 75th percentiles. **(C)** Fresh and **(D)** dry weight of storage roots. Dry weight of cassava storage roots consists of approximately 80% starch. No significant differences were detected for any trait measured (1-way ANOVA, $p > 0.05$). **(E)** Representative image of fresh storage root cross-section. Scale bar = 1.0 cm.

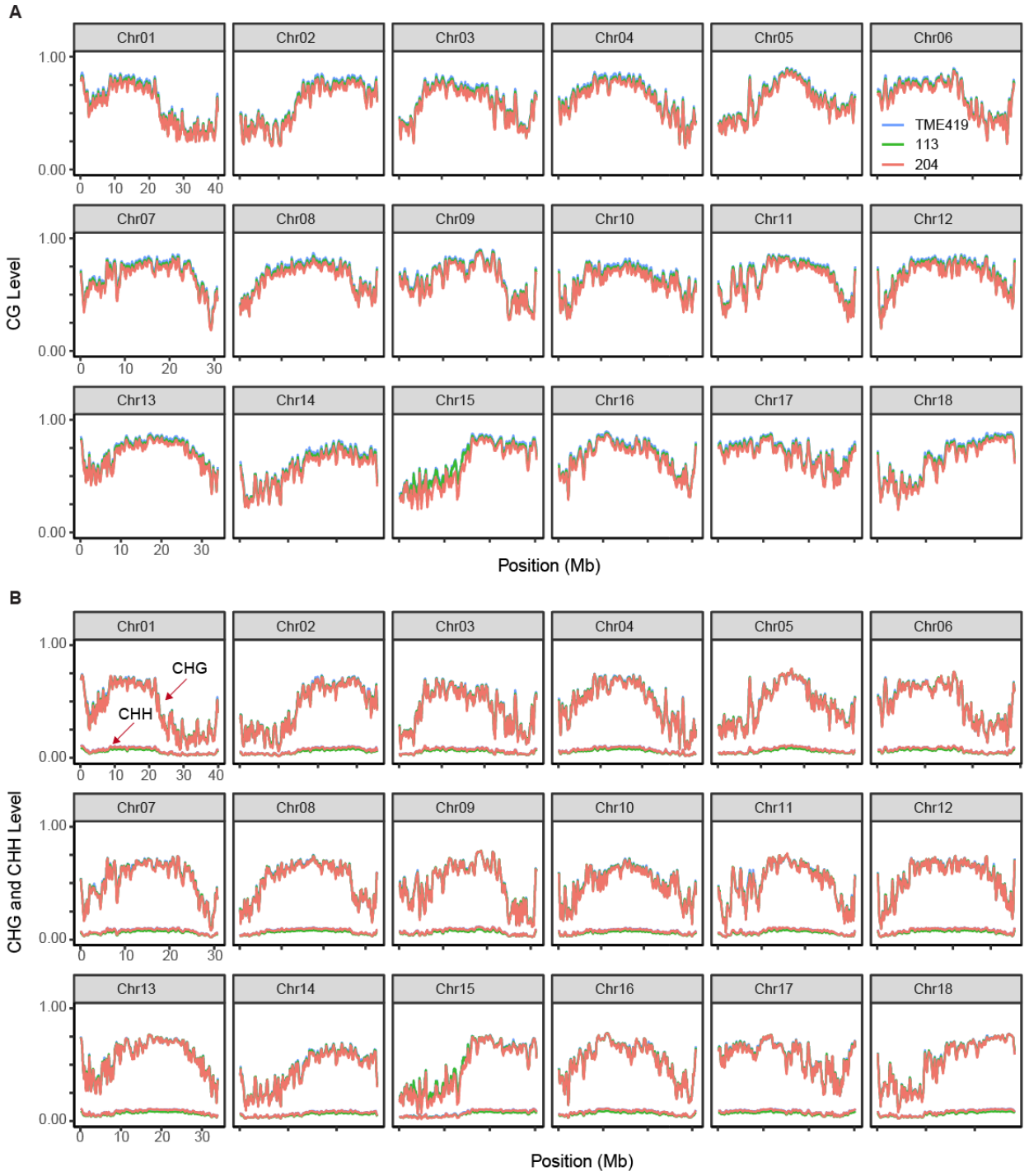

Fig. S9. – Genome-wide DNA methylation of chromosomes.

Genome-wide distribution of **(A)** CpG, **(B)** CHG, and CHH methylation over 18 Cassava chromosomes in wild-type TME419 and two independent DMS3-ZF lines (133 and 204). Methylation levels were calculated by splitting chromosomal sequences into 100 kb bins.

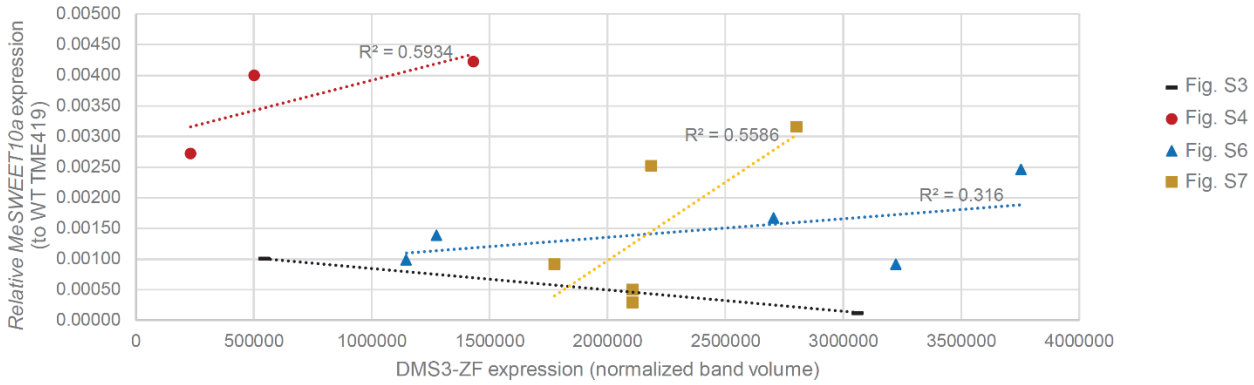

Fig. S10. – DMS3-ZF expression does not correlate with reduced *MeSWEET10a* induction. All *MeSWEET10a* expression values (y-axis) from Fig. 4 (*Xam*-treated leaves) plotted against the DMS3-ZF expression level quantified in **Fig. S3, S4, S6,** and **S7** (qPCR experiments 1-4). The legend (right) identifies each experiment. R^2 values indicate a lack of correlation for each experimental set, where applicable.

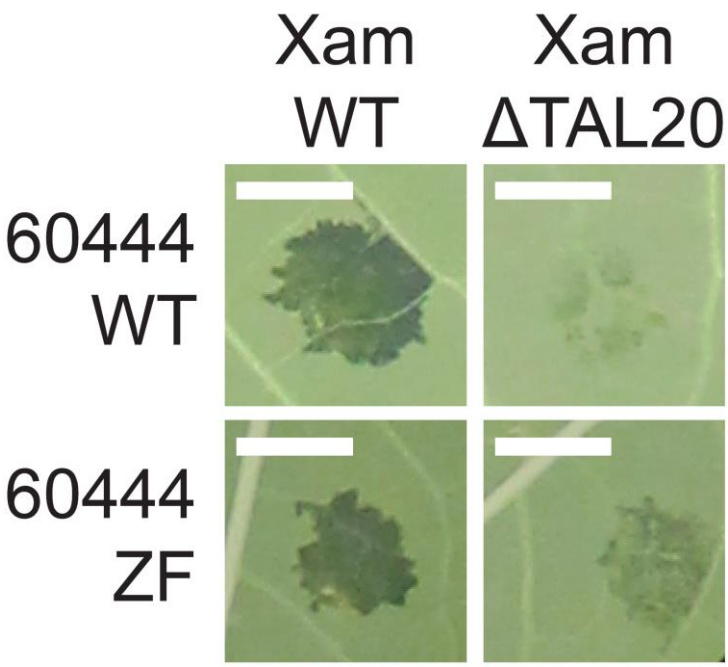

Fig. S11. – Phenotype of additional *Xam*-infiltrated control plants.

Representative images of water-soaking phenotype of leaves from 60444 wild-type (WT) and ZF negative control plants. Images were taken 4 days post-infection with either *Xam668* (XamWT) or a *Xam668* TAL20 deletion mutant (XamΔTAL20). Scale bar = 0.5 cm.

Primer Number	Primer Name	Sequence (5'-3')	Description
107	Manes.09G039900_Me PP2A-4 NTv2_For	AGGCTCACACTTTCATCCAGTTTGAG	RT-qPCR
108	Manes.09G039900_Me PP2A-4 NTv2_Rev	ACCTGAGCGTAAAGCAGGGAAG	RT-qPCR
109	GTPb (Manes.09G086600)_For	CCTCAAAGGCTGAGCCACAGA	RT-qPCR
110	GTPb (Manes.09G086600)_Rev	GGGAGAAACAATACAGGCACCAATCAC	RT-qPCR
348	10a_qPCR-F3	GCGGTGATGTGGTTCTTC	RT-qPCR
349	10a_qPCR-R3	CGATGTGCTCGGACAATTC	RT-qPCR
117	Manes.15G048700_qPCR-F3	CCTGGTTGATGCTGTCATGGG	RT-qPCR
119	Manes.15G048700_qPCR-R4	GGTGGGATTTGCACTTCCACC	RT-qPCR
120	JP16889	ATATTGTTTTTTTTTTTTTTAAAAAAAATAATAAAAGAAATAAGGTT	ampBS-seq
121	JP16890	TCCRACTATAATAAAAACTCTCTTTCCCTTA	ampBS-seq

Table S1. - Primers used to generate data presented in this manuscript.

Each primer has a number and a name (first two columns). Column 3: the sequence of the primer (5’ to 3’ direction). Column 4: How primer was used.

1